



# LUND UNIVERSITY

## Modeling and Identification of a Nuclear Reactor

Olsson, Gustaf

1975

*Document Version:*

Publisher's PDF, also known as Version of record

[Link to publication](#)

*Citation for published version (APA):*

Olsson, G. (1975). *Modeling and Identification of a Nuclear Reactor*. (Technical Reports TFRT-7075). Department of Automatic Control, Lund Institute of Technology (LTH).

*Total number of authors:*

1

### General rights

Unless other specific re-use rights are stated the following general rights apply:

Copyright and moral rights for the publications made accessible in the public portal are retained by the authors and/or other copyright owners and it is a condition of accessing publications that users recognise and abide by the legal requirements associated with these rights.

- Users may download and print one copy of any publication from the public portal for the purpose of private study or research.
- You may not further distribute the material or use it for any profit-making activity or commercial gain
- You may freely distribute the URL identifying the publication in the public portal

Read more about Creative commons licenses: <https://creativecommons.org/licenses/>

### Take down policy

If you believe that this document breaches copyright please contact us providing details, and we will remove access to the work immediately and investigate your claim.

LUND UNIVERSITY

PO Box 117  
221 00 Lund  
+46 46-222 00 00

TFRT-7075

MODELING AND IDENTIFICATION OF A  
NUCLEAR REACTOR

G. OLSSON

Report 7504 (C) Februari 1975  
Lund Institute of Technology  
Department of Automatic Control

## Chapter

### MODELING AND IDENTIFICATION OF A NUCLEAR REACTOR

Gustaf Olsson

Department of Automatic Control

Lund Institute of Technology

S-22007 Lund, Sweden

- I. INTRODUCTION
- II. DESCRIPTION OF THE NUCLEAR REACTOR
  - A. Plant Description
  - B. Reactivity Feedbacks
  - C. Step Responses
- III. EXPERIMENTS
  - A. Summary of the Experiments
  - B. Internal Controllers
  - C. Experimental Design Considerations
  - D. Instruments and Actuators
- IV. IDENTIFICATION METHODS
  - A. Multiple-Input-Single-Output Structure
  - B. Multivariable Structures
  - C. A Vector Difference Equation Approach
  - D. Recursive Parameter Estimation
  - E. Model Verification
  - F. Computational Aspects

- V. MULTIPLE-INPUT - SINGLE-OUTPUT MODELS
  - A. Nuclear Power
  - B. Primary Pressure
  - C. Secondary and Tertiary Pressures
  - D. The Problem of Negative Real Discrete Poles
- VI. VECTOR DIFFERENCE EQUATIONS
  - A. Correlation Analysis
  - B. Maximum Likelihood (ML) Identifications
  - C. Simulations
- VII. A STATE MODEL
  - A. Derivation of a Model Structure
  - B. Parameter Identification
- VIII. RECURSIVE IDENTIFICATION
  - A. Influence of Subcooling Power
  - B. Parameter Tracking

#### ACKNOWLEDGEMENTS

#### REFERENCES

The purpose of this paper is to find linear stochastic models of different structures for a nuclear reactor. The models will be used for control. The results are based on experiments performed on the Halden Boiling Water Reactor (HBWR), Norway, in cooperation with the OECD Halden Reactor Project. The plant is considered a multivariable sys-

tem. Spatial effects are neglected. Three inputs have been used in the experiments. Problems relating to experimental design, data preparation, choice of model structure, identification methods, computations and model verifications are considered. The dynamics of the reactor is briefly described, and the identification results are compared to theoretical or empirical experiences. Maximum Likelihood technique is used predominantly for parameter estimation.

## I. INTRODUCTION

Some representative results from modeling and identification experiments on the Halden Boiling Water Reactor, (HBWR), Norway, are presented in this paper. Linear input-output models as well as time invariant and time variable linear state models have been used as model structures. Some of the results are presented previously in [1 - 3], while others are new.

The purpose of the paper is to describe the different phases of identification and modeling of a complex dynamical system. Different identification methods have been used to demonstrate the applicability of identification technique as a tool to explore the dynamics of a nuclear reactor.

A nuclear reactor is an example of a very complex dynamical system and offers some special features. There is a wide span of time constants in the system. The neutron kinetics is very fast, and the dominating kinetics time constant is about 0.1 second. The typical time constants for actuators and instrument dynamics vary between fractions of a second and about one second. The fuel element heat dynamics are of the order of a few seconds. The heat transfer in moderator and coolant channels as well as the hydraulics is of the order of some seconds up to

some minute. The heat transfer through the heat removal circuits will take one to several minutes. Xenon oscillations have a time period of the order of days. On an even longer time scale there are the burn out phenomena due to fuel consumption.

Several nonlinear phenomena are important in a nuclear reactor. The dynamics of the coolant channels are very complex. The relation between boiling boundary, void contents and reactivity is generally highly nonlinear and very difficult to model. The heat exchanger dynamics and steam generation are also significantly nonlinear.

Many phenomena are spatially dependent. Power distribution oscillations due to xenon are not negligible in a large reactor. The spatial variations of void content and temperature in the coolant channels are essential, dynamical phenomena. The neutron distribution is not homogeneous since the fuel elements are burnt out at different rates in different parts of the core.

A model used for controller design cannot include all the mentioned phenomena in detail. A large number of compromises must be made in order to make the model not too large and still accurate. The purpose of this paper has primarily been to find linear models for steady state control. The nuclear power and the primary pressure then are the most important outputs to be controlled. This li-

mits the interesting span of time constants to be smaller than some minutes. The results of the investigation show that the dynamics of the reactor generally can be described by quite low order models. It will be demonstrated that identification is a useful tool to find simpler descriptions of such a complex process.

Modeling and identification problems for nuclear power reactors have been considered extensively. The Maximum Likelihood (ML) method is compared with other methods for a reactivity-nuclear power model by Gustavsson [4]. Sage et al [5] use a least squares approach to identify parameters in a reactor model. Ciechanowicz et al [6] use spectral analysis to identify parameters in a simple linear model. Recursive identification or parameter tracking has been reported by different authors. Habegger et al [7] apply Extended Kalman techniques to track parameters in a nuclear system. Moore et al [8] use a combination of least squares and ML approach to get an adaptive control scheme of a model of a pressurized water reactor.

The dynamics of the Halden reactor has been studied extensively before. Single input experiments have been performed, e.g. step response analysis by Brouwers [9], frequency analysis by Tosi et al [10], pseudo random reactivity perturbation experiments by Fishman [11] and



noise experiments by Euroola [12]. Bjørlo et al [13] have reported a linear multivariable model of the HBWR. The vessel pressure dynamics and core dynamics have been studied with recursive least squares techniques by Roggenbauer [14].

Four different approaches to the model building techniques are investigated in this report:

- o multiple-input - single-output models with no *a priori* assumption about physical behaviour,
- o multivariable (vector difference) models without physical *a priori* knowledge,
- o estimation of parameters in linear time invariant state models with known structure and *a priori* noise structure assumptions,
- o estimation of time variable parameters in linear stochastic state models.

It is natural that a model with no *a priori* assumption about the physics does not demand physical insight into the process, at least not to get parameter values. In general there is no physical interpretation of the parameters, and it is therefore sometimes difficult to verify the models in more general terms. On the other hand, such a model can give a good insight into the required com-

plexity of a more structured model. The validity of the model is limited to the same operational conditions for the plant as those during the identification experiment.

As a nuclear reactor is a multivariable system, the second approach is an attempt to take the couplings of the system into consideration without too many *a priori* assumptions. Compromises about the noise have to be made. The approach gives a better idea of the couplings in the system, and it is then easier to derive reasonable structures for more advanced models.

A state model with some of the parameters unknown naturally requires more insight into the process. In such a model the parameters have physical interpretations. If the assumptions on the structure are perfect, the model accuracy can be high. On the other hand, if the assumptions are imperfect, the model can be more inaccurate than an input-output model without *a priori* assumptions. The identification would then be constrained into too few degrees of freedom, either because of too few free parameters or of a wrong *a priori* structure.

In order to be valid for varying operating conditions the plant model should be nonlinear. Alternatively it has here been assumed a time varying linear state model. Some of the variable parameters then have been tracked

by recursive identification techniques.

The paper is organized as follows. In section II, the reactor plant is described and its dynamics are studied qualitatively. A summary of the experiments selected is made in section III. Experimental design is also considered, as well as instrumentation and actuator characteristics. The identification methods used are briefly presented in section IV. Maximum likelihood identification technique has been applied predominantly. The multiple-input - single-output models are discussed in section V. Although accurate models were found, the linearity of the models is a limitation, and it is doubtful if they are valid in a large operational range. Improvements of the accuracy were obtained by introducing other couplings by a vector difference equation approach in section VI. In chapter VII a linear state vector model structure is presented. Parameters of this structure are identified. The recursive parameter tracking is finally described briefly in section VIII.

## II. DESCRIPTION OF THE NUCLEAR REACTOR.

A short description of the reactor is given to provide a physical background. In the first paragraph the different parts of the plant are briefly described. In paragraph B the most important dynamical reactivity feedbacks are considered. Finally it is discussed how changes in the three actual inputs propagate through the system.

### A. Plant Description.

The reactor plant has been described elsewhere in great detail, e.g. in Jamne et al [15] and several other reports from the Halden Reactor Project, e.g. [9 - 13]. For easy reference some main features of the plant are described here.

A simplified sketch of the plant with its heat removal circuits is shown in Fig. 1. The HBWR is a natural circulation, boiling heavy water reactor. It can be operated at power levels up to 25 MW and at 240°C.

#### 1. Core and Primary Circuit.

In the primary circuit heavy water is circulated in a closed loop. This circuit consists of the reactor vessel, steam transformers and a subcooler A. The latter ones

are heat exchangers for the steam and water circulation loops respectively.

The core consists of enriched uranium fuel moderated by heavy water. There are 100 fuel assemblies in the core arranged in a hexagonal pattern each element being 88 cm in length. The core diameter is 167 cm and is surrounded by a radial reflector with a thickness 51 cm. The bottom reflector is 38 cm thick.

The fuel elements in the core have shrouds into which heavy water from the moderator enters through the holes in the bottom section. The shrouds create a defined flow pattern, and can separate the upstreaming mixture of steam and water from the downstreaming water between the elements. The lower part of the core is not boiling while the upper part is. The water in the system is close to the saturation temperature.

The mixture of steam and water leaves the shrouds through holes at the top and separation of water and steam takes place. The steam passes from the reactor vessel through the primary side of a heat exchanger called the steam transformer. As the steam is condensed it is pumped together with water from the bulk of the moderator through the primary side of the subcooler A (Figs. 1, 2). The water

is cooled a few degrees below the saturation temperature and then recirculated into the vessel.

The reactivity is controlled by 30 absorbtion rods which can be inserted into the core.

## 2. Subcooling Circuit.

The mass flow of subcooled water is controlled by a valve  $u_1$  (VA 770). As the subcooled water enters the moderator it mainly affects the moderator temperature. The main purpose of the subcooling circuit is to suppress boiling of the moderator. To a lower extent it controls the reactivity of the core.

The water loop is to some extent similar to the coolant flow circulation system in a light water BWR, even if there are major differences. In the HBWR this system is not primarily designed for control purposes, and thus the flow and also the reactivity feedback are much smaller than in a light water BWR. The void reactivity feedback is about 20 pcm/% void ( $1 \text{ pcm} = 10^{-5}$ ) in the HBWR compared to about 125 pcm/% void in a BWR.

Because of the limited control authority of the valve  $u_1$  it cannot alone control the nuclear power in the HBWR over a wide range as compared to a light water BWR. It must be complemented by the absorbtion rods.

### 3. Secondary and Tertiary Circuits.

The secondary circuit is closed and filled with light water (see Figs. 1, 2). Water coming from the steam drum is circulated through the secondary side of the steam transformer and back to the steam drum. The secondary circuit also includes a steam flow from the steam drum to the primary side of a steam generator where it is condensed.

The condensed water returns via the hot well to the subcooler B, where primarily feedwater is preheated. The water is further heated up in the subcooler A before it returns to the steam drum. This steam drum mainly serves as a separator for steam and water.

The tertiary circuit is an open loop circuit of light water. The water is heated up to form steam in the secondary side of the steam generator. The steam can be used by consumers through a valve  $u_2$  (VB 282). The plant has no turbine, but  $u_2$  should normally be the turbine controller. The steam can be recirculated via the feedwater tank and the subcooler B to the steam generator.

### B. Reactivity Feedbacks

The essential part of the dynamics has to do with the reactivity feedbacks. For the discussion we refer to Fig. 3. The net reactivity determines the nuclear power which is produced in the core. This net reactivity is a sum of several feedback effects. The nuclear power is created through the fission, which can be described by the kinetic equations, including delayed neutrons. This power generates heat which is transferred through the fuel elements. A change in fuel temperature causes a negative reactivity feedback. The heat flux transfers heat via the fuel elements and the moderator into the coolant. The moderator dynamics describes the temperature and void distribution in the moderator. It is related to the steam pressure, and water and steam velocities.

It should be remarked that there are some important differences between light water and heavy water boiling reactors. In  $H_2O$  systems almost all the moderator is boiling. In  $D_2O$  systems the boiling takes place only in a fraction of the moderator space, because the moderator-to-fuel ratio is relatively large. Therefore models of light water boiling reactors, which are described in the literature, such as Fleck [16], differ from the HBWR in basic assumptions.



The heat flux consists of several components. Except the nuclear power it is determined by gamma and neutron heating as well as the subcooling power. The coolant channel dynamics (the void and temperature distributions in the coolant channels) is primarily determined by the heat flux, but also by the vessel pressure, the steam and water velocities as well as the channel inlet temperature. This one in turn depends on the moderator temperature. Naturally those phenomena are spatially dependent. Therefore it should be emphasized, that not only the total heat flux but also the spatial distributions of void contents, water velocities and neutron flux distribution will certainly influence the total power. If the model should include all those phenomena, however, it would be too complex for control purposes. Therefore the variables are weighted over the space, and some crucial assumptions, especially about the hydraulics, have to be made. Because of this, it is also in some cases difficult to give a physical explanation of certain parameters, as they in essence are combinations of several microscopic coefficients. The reactivity feedbacks from temperatures and void contents are crucial for the total plant behaviour. The physical explanation for reactivity couplings can be studied in standard textbooks, like Glasstone-Edlund [17], King [18], Meghreblian-Holmes [19], Weaver [20].

Another important reactivity feedback has to do with fission products with extremely high neutron absorption, such as xenon. Transients due to xenon can appear in two ways. One type of xenon transients appears at high neutron flux levels and is enforced due to power changes. This varies the average concentration of xenon, and consequently the neutron level. As all the experiments have been performed at almost constant power, no such power transients are actual.

The other type of xenon feedback occurs in reactors with large geometrical dimensions. There the xenon concentration can oscillate spatially between different parts of the core, thus creating hot spots of power, while the average power is constant. Such phenomena have been analyzed by several authors, e.g. Wiberg [21] and Olsson [22] and will not be considered here because of two reasons. First, the oscillations are too slow to be of interest here, as the primary purpose is to keep nuclear power and primary pressure constant. Second, the Halden reactor has small geometrical dimensions so that the spatial oscillations are too much damped to be of any interest.

The essential disturbances to the system consist of reactivity perturbations from the absorption rods or changes

in the steam consumption.

A quite comprehensive description of the details of the HBWR dynamics can be found in Vollmer et al [23] and Eurola [24].

### C. Step Responses.

For the following discussion it is useful to have an overview of the major physical phenomena of the plant. The purpose is to provide this by qualitative discussion of step responses and the major physical phenomena that are involved. The results are based on both theoretical considerations and practical experiences.

#### 1. Subcooling Valve $u_1$ .

Assume that the valve  $u_1$  (VA 770) is closed stepwise. As only small changes are discussed linear relations are assumed. The downcomer subcooled flow  $F_6$  (see Figs. 2, 4) decreases rapidly as the valve closes. The water temperature  $T_{100}$  just before the subcooler is not affected, but the subcooled water flow temperature  $T_8$  is decreased with a few seconds time constant (Fig. 4).

The heat flow delivered to the subcooler A is called the subcooling power  $Q$ . This power is calculated from energy balances over the heat exchanger (subcooler A) and is a

function of the product of the temperature change of T8 and the flow change of F6.

It is possible to empirically relate the subcooling power in a simple fashion, to F6, T8 and  $u_1$ , as can be visualized by Fig. 4. As the flow F6 is closely related to the valve opening  $u_1$ , the subcooling power change can be written

$$\delta Q(s) = a_1 \delta(T8(s)) + a_2 \frac{1}{1 + Ts} \delta(u_1(s))$$

where  $s$  is the Laplace operator.

The subcooling power can also empirically be written as a function of T8:

$$\delta Q(t) = \alpha_1 \delta(T8) + \alpha_2 \frac{d(T8)}{dt}$$

where  $\alpha_1 > 0$ ,  $\alpha_2 > 0$ .

The effect of closing the valve is thus, that more heat energy is returned to the core. The bubble formation in the moderator is amplified, and this phenomenon directly causes a negative reactivity feedback. Because of this the nuclear power decreases quite rapidly.

In a longer time scale several secondary effects take place, which is illustrated by the step response in Fig. 5. As the nuclear power decreases, the vessel pressure and the temperatures also decrease. Other reactivity feedbacks now are beginning to act and the nuclear power is slowly returned to a more positive value.

The vessel pressure naturally is coupled through the steam transformer to the secondary and the tertiary circuits. Those pressures therefore slowly follow the pressure decrease in the vessel. The steam production in the primary circuit is, however, influenced to a lesser degree.

When  $u_1$  is closed only a slight decrease of the steam inlet flow F41 (Fig. 2) can be observed. The same is true for the flow F28 in the secondary circuit.

## 2. Consumers Steam Valve $u_2$ .

A sudden increase of the valve opening  $u_2$  (VB 282) for the tertiary steam flow directly increases the tertiary steam flow F21 (see Figs. 6 and 2). Consequently the tertiary pressure (P62) will be decreased with a dominating time constant of about one minute.

The temperature T55 is strongly coupled to the pres-

sure variations and it follows the pressure P62 closely. Also the flow F16 is increased, but delayed a few seconds after the flow F21. The feedwater temperatures T60 and T61 are quite unaffected by  $u_2$ .

When the heat flow through the secondary side of the steam generator is decreased also the secondary pressure P61 will decrease (Fig. 6). The temperature T18 is closely coupled to the pressure and follows P61 quite well. The hot well temperature T57 and the secondary water temperature T81 are relatively constant despite changes in  $u_2$ .

The flows F27 and F28 are varying quite noticeably. The dynamics is, however, significantly influenced by an internal controller. The hot well level is kept constant in all the experiments by a valve controlling the flow F28. The flows F27 and F28 increase when the valve  $u_2$  is opened.

The pressure drop in the tertiary and secondary circuits is propagated to the primary circuit with a 2-3 minutes' time delay, and thus the vessel pressure P13 is decreased (Fig. 6). A pressure drop in the core will cause the void to increase in the first moment, and the boiling boundary will fall. The reactivity feedback from void therefore has the effect to decrease the nuclear power in the first moment. When the power decreases, however, the steam

production also decreases, thus creating a smaller void content and a higher boiling boundary again. This causes the nuclear power to increase. As indicated by the experimental step response in Fig. 7 the nuclear power shows a non minimum phase behaviour.

The control power from  $u_2$  is significantly larger than that of  $u_1$ , a fact which is illustrated by the step responses in Figs. 5 and 7. On the other hand, the valve  $u_1$  can change the nuclear power much more rapidly than the valve  $u_2$ , so they complement each other dynamically. In a light water BWR, as mentioned before, there is not such a great difference in control authority between  $u_1$  and  $u_2$ .

From an identification point of view the valve  $u_2$  is certainly the best input for studies of the heat removal circuit dynamics. The valve  $u_1$  naturally has the strongest influence on the subcooling circuit.

### 3. Control Rod Reactivity $u_3$ .

By inserting or withdrawing the absorbtion rods the nuclear power can be rapidly and significantly changed. This dynamics is very rapid and is governed mainly by the delayed neutrons. If the rods are properly positioned, so that the reactivity change per step is large enough, the rods can control the nuclear power very well. It should be observed, however, that also the flux distribution ge-

nerally is affected by the rods. Moreover, wearing out problems should be considered, which means that the rods should not be used for frequent control movements.

The nuclear power transfers heat to the fuel elements quite rapidly with a time constant of the order 5-10 seconds. The temperatures of the moderator and coolant increase more slowly. The pressure changes are quite slow, of the order half a minute for the vessel pressure to about a few minutes for the tertiary pressure.

### III. EXPERIMENTS.

In this section we will consider experimental design problems, such as choice of input signals and measurements. The selected experiments are summarized and the data handling problems are mentioned. In all the experiments the input disturbances were generated in the IBM 1800 computer, connected to the plant. All measurements were also registered using the computer.



### A. Summary of the Experiments.

In table 1 the main features of the operating conditions are shown for the selected experiments.

TABLE 1  
Summary of the identification experiments

Exp	$u_1$ (%) VA770	$u_2$ (%) VB282	$u_3$ (steps) Rods	Nuclear power (MW)	Subcooling power (MW)
1	-	-	3 (13,15,17)	9.7	1.35
2	-	-	3 (13,17,18)	9.95	1.85
3	-	$\pm 2.5$	3 (13,17,18)	10	1.95
4	-	$\pm 3$	2 (20,21)	10	1.95
5	$\pm 7$	$\pm 3$	-	10	2.0
6	-	$\pm 2$	1 (20)	8.0	1.1
7	-	$\pm 2.5$	2 (20,21)	10.0	1.95-1.35

The valve amplitudes are defined in % opening. The reactivity is defined in "steps", where one step reactivity is defined as the reactivity corresponding to the movement of the rod step motors one step. It corresponds to 7-10 pcm reactivity, depending on the position of the rods. The figures in brackets under  $u_3$  in table 1 define the rod numbers. The rods are moved in parallel one step up and down.

Most of the experiments contain more than 3000 samples, i.e. 6000 seconds. For identification purposes not more than 2000 samples have been used at the time.

For safety reasons it was sometimes necessary to move some control rod manually in order to keep the nuclear power and vessel pressure within permitted limits.

#### B. Internal Controllers.

It was important to study the plant in open loop operation, and therefore some controllers were removed, primarily the nuclear power controller, which keeps the nuclear power within desired limits by adjusting the absorption rods.

The primary (vessel) pressure is controlled by a PID controller acting on the valve  $u_2$  (VB 282). For safety reasons it was not allowed to remove this control in the first experiment series, here represented by experiment 1. As this control loop has a time constant of more than one minute, the fast time constants still could be determined. When more experiences had been gained, it was allowed to remove also the pressure controller, experiments 2-7.

Other local controllers were acting as before, i.e.

control of the hot well level and steam generator level as well as return flow to the feedwater tank. These controllers, however, do not influence the determination of the overall dynamics.

### C. Experimental Design Considerations.

In the design of input signals and operating levels a large number of conditions have to be considered. A general survey of such problems have been described in Gustavsson [25].

In order to gain a good signal-to-noise ratio a large input amplitude is desired. Through preliminary experiments it was found, that three rods moved one step in parallel could disturb the nuclear power about 0.5 MW from the operating level of about 10 MW. The upper limit of the changes in  $u_1$ ,  $u_2$  and  $u_3$  were determined by nonlinear effects.

One experiment was done in order to cover a wider range of operational conditions, expt. 7. The subcooling power was changed along a desired ramp. The parameters of a time variable model then were identified recursively (see VIII).

The major time constants were discussed in I and II. They will determine the desired frequency content of the input signals. The upper limit of the frequency was deter-

mined by practical reasons, as the computer sampling time was fixed to 2 seconds. By experience we also know, that in one identification experiment it is difficult to accurately determine time constants spanning more than about 2 decades, i.e. here from some second to a few minutes.

In all the reported experiments pseudo random binary sequences (PRBS) have been applied as inputs as it was desirable to get persistently exciting signals. In the case of several inputs, the signals have been chosen so as to be independent. As the pressure control was in action in expt. 1, the input signal was chosen to excite time constants essentially smaller than one minute. In experiments 2-7 the sequence was chosen with longer pulses in order to get better estimation of the long time constants.

There are different rules of thumb in the literature how to choose a suitable PRBS sequence, and those rules can give quite different results, as demonstrated here. Briggs et al [26] have made a detailed analysis of the PRBS sequence. According to their rules the period time of the sequence should be at least 5 times the longest time constant  $T_m$  of the process. Another rule of thumb says, that the longest pulse of the sequence should be at least  $3 \cdot T_m$ . Then the process is allowed to reach a new steady state during the pulse, and the estimation of the gain and largest time constant will be improved. The PRBS sequence for expt. 1

was chosen with the shortest pulse length of 2 seconds, a period time of 991 samples (almost 2000 seconds) and a longest pulse length of only 18 seconds. With the cited rules applied to this sequence it limits the longest time constant either to 400 seconds or to 6 seconds, a significant difference. Thus it is found that the PRBS sequence can be too fast for the low frequencies. This fact has been observed also e.g. by Gustavsson [25] and Cumming [27], [28].

For the second PRBS sequence the period time is still about 2000 seconds but the longest pulse is 196 seconds. According to the referred rules the longest time constant then could be 60-400 seconds. The shortest pulse was chosen 12 seconds, but still the sampling time is 2 seconds. It is shown in section V, that the sampling time - and not only the input sequence - is important for the accuracy of the long time constants.

#### D. Instruments and Actuators.

The variables recorded during the experiments are indicated in Fig. 2. The meaning of the letters are

- P - pressure
- F - steam or water flow
- T - temperature
- C - nuclear power

The HBWR instrumentation is described in detail elsewhere, see [29]. Here only the main features are summarized. The pressures are registered as differential pressures in the three circuits (P13, P61, P62) with conventional DP cells with a range of about  $\pm 0.3$  bar.

The flows are generally measured with venturi meters plus differential pressure cells. The temperatures are measured by thermocouples. The nuclear power is measured by an ion chamber C10.

The pressure cells and flow meters in the primary circuit have time constants around one second. The temperatures, however, are registered much faster, at about 0.1 second. The instrumentation does not generally cause any problem, as the important dynamics generally are much slower. The actuator time constants are not negligible. To move a valve through its whole range takes about 6 seconds. A typical time delay for the valve  $u_1$  in the experiments was therefore about 1 second. For the valve  $u_2$  the corresponding delay was about half a second.

The instrument noise of the pressure meters and the nuclear channel are well known from previous experiments, see e.g. [9 - 12]. For the nuclear power the measurement noise is about  $\pm 0.03$  MW. The standard deviation for the differential pressure meters has also been experimentally determined.

Typical values are  $0.5 \cdot 10^{-4}$  units. The pressure unit is expressed as pressure variation divided by total pressure. During the experiments the total variation of e.g. the vessel pressure was about  $\pm 0.5 \cdot 10^{-2}$  units. This means, that the noise to signal ratio was about 1%.

The A/D converter has 11 bit resolution, and conversion errors must be considered. For the nuclear power measurements the total power is measured and converted. As the power variations are most about 5% of the total power the conversion errors are not negligible, especially for long input pulses, when the variations of the signal are small. The error is estimated to be about  $5 \cdot 10^{-3}$  MW. The quantization errors must also be considered for the pressure meters, see V.D.

During the experiments 35 variables were recorded, some of them only for checking up purposes. The data were logged on the IBM 1800 computer and were measured with 2 seconds sampling interval by a 100 Hz relay multiplexer. Because of the multiplexer the measurements could be up to 0.3 seconds separated in time for the same sampling interval. The sample and hold circuit also introduced a time constant, about 0.35 sec.

#### IV. IDENTIFICATION METHODS.

For the preliminary analysis of the experimental data and for the first model approaches simple methods were used to find rough estimates of the input-output relationships. Step response analysis and correlation analysis were used to verify preliminary models and to design new experiments. For the parameter estimation the Maximum Likelihood method has been used except for the recursive estimation, where an Extended Kalman filter is applied.

In this section the methods are summarized. For detailed descriptions a large number of papers are available, see e.g. Åström-Eykhoﬀ [30], Eykhoﬀ [31], and Mehra et al [32].

##### A. Multiple-Input-Single-Output (MISO) Structure.

The plant dynamics is represented by the canonical form, introduced by Åström et al [33]

$$(1 + a_1 q^{-1} + \dots + a_n q^{-n}) y(t) = \sum_{i=1}^p (b_{i1} q^{-1} + \dots + b_{in} q^{-n}) \cdot u_i(t) + \lambda(1 + c_1 q^{-1} + \dots + c_n q^{-n}) e(t)$$

or

$$A^*(q^{-1}) y(t) = \sum_{i=1}^p B_i^*(q^{-1}) u_i(t) + \lambda C^*(q^{-1}) e(t) \quad (1)$$



where  $q$  is the shift operator and  $p$  the number of inputs.  $A^*$ ,  $B^*$  and  $C^*$  are defined as corresponding polynomials in  $q^{-1}$ . It is trivial to extend the model to include both time delays and direct input terms, corresponding to a coefficient  $b_{i0}$  in (1). Moreover initial conditions can be estimated.

If  $e(t)$  is assumed to be a sequence of independent gaussian random variables the parameters  $a_i$ ,  $b_i$ ,  $c_i$  and  $\lambda$  can be determined using the method of Maximum Likelihood (ML). The method is described in detail elsewhere, e.g. [30 - 33], and only some remarks will be made here.

The likelihood function  $L(\theta; \lambda)$  for the unknown parameters

$$\theta^T = (a_1 \ a_2 \ \dots \ a_n \ b_{11} \ \dots \ b_{pn} \ c_1 \ \dots \ c_n) \quad (2)$$

is given by

$$\ln L(\theta; \lambda) = - \frac{1}{2} \sum_{i=1}^N \frac{1}{\lambda^2} \varepsilon^2 - N \ln \lambda + \text{const.} \quad (3)$$

where the residuals  $\varepsilon(t)$  are defined by

$$\varepsilon(t) = [\hat{C}^*(q^{-1})]^{-1} [\hat{A}^*(q^{-1})\hat{Y}(t) - \sum_{i=1}^p \hat{B}_i^*(q^{-1})u_i(t)]$$

and  $\hat{A}^*$ ,  $\hat{B}_1^*$  and  $\hat{C}^*$  are estimates of the polynomials  $A^*$ ,  $B_1^*$  and  $C^*$ .  $N$  is the number of samples and  $\lambda^2$  is the covariance of the residuals.

The maximization problem reduces to the problem of minimizing the loss function

$$V = \frac{1}{2} \sum_{t=1}^N \epsilon^2(t) \quad (4)$$

with respect to the unknown parameters. When the estimate  $\hat{\theta}$  is calculated the parameter  $\lambda$  can be solved from the minimum value of the loss function

$$\hat{\lambda}^2 = \frac{2}{N} V(\hat{\theta}) \quad (5)$$

In [33] it is shown that the estimates are consistent, asymptotically normal and efficient under quite mild conditions. The parameter  $\lambda$  can be interpreted as the standard deviation of the one step prediction error. The technique gives not only the estimates but also their standard deviations from the Cramér-Rao inequality.

As the number of parameters in the model or the system order is not given a priori a statistical test can be done

in order to find the proper model. The loss function should not decrease significantly if the right order has been reached and more parameters are added. It is shown in [33] that the quantity

$$F_{n_1, n_2} = \frac{V_{n_1} - V_{n_2}}{V_{n_2}} \cdot \frac{N - n_2}{n_2 - n_1} ; \quad n_2 > n_1 \quad (6)$$

asymptotically has an F-distribution, where  $n_i$  is the number of parameters and  $V_{n_i}$  the corresponding loss functions. The residuals should also be tested for independence in time and in relation to the inputs.

An alternative test function due to Akaike [34] has also been used besides the F test. An Information Criterion is defined,

$$J = \frac{N + k}{N - k} \ln |\lambda^2| \quad (7)$$

where  $N$  is the number of samples,  $k$  the number of parameters and  $\lambda^2$  the measurement noise covariance. Typically  $J$  as a function of  $k$  has a minimum for the right number of parameters.

The ML identification method has been extensively used in a large number of applications. Surveys are given in [25],

[30] and [32].

### B. Multivariable Structures.

The ML method has been generalized to the multivariable case. It is desirable to estimate a parameter vector  $\theta$  of a linear continuous model

$$dx = Axdt + Bu dt + dv \quad (8)$$

$$dy = Cxdt + Du dt + de \quad (9)$$

The model is written in discrete time and in innovations form in order to simplify the noise estimation, according to Åström [35] or Mehra [36],

$$\begin{aligned} \hat{x}(t+1) &= \phi \hat{x}(t) + \Gamma u(t) + K \varepsilon(t) \\ y(t) &= C \hat{x}(t) + Du(t) + \varepsilon(t) \end{aligned} \quad (10)$$

where

$$\begin{aligned} \phi &= e^{A(\theta)} \\ \Gamma &= \left\{ \int_0^1 e^{A(\theta)s} ds \right\} B(\theta) \end{aligned}$$

and  $\hat{x}(t)$  denotes the conditional mean of  $x(t)$ , given previous measurement values  $y(t-1), y(t-2), \dots$

The noise  $\varepsilon(t)$  is now a sequence of independent gaussian random vector variables. The likelihood function (3) is generalized to the form

$$\begin{aligned} \ln L(\theta, R) = & -\frac{1}{2} \sum_{t=1}^N \varepsilon^T(t) R^{-1} \varepsilon(t) - \\ & -\frac{N}{2} \ln \det R + \text{const} \end{aligned} \quad (11)$$

where  $R$  is the covariance of  $\varepsilon(t)$  and is assumed to be constant. The loss function (cf. (4)) is

$$V = \det \left| \sum_{t=1}^N \varepsilon(t) \varepsilon^T(t) \right| \quad (12)$$

Eaton [37] has shown that the loss function can be minimized independently of  $R$ . As soon as the minimum of  $V$  is found an estimate of  $R$  can be achieved,

$$\hat{R} = \frac{1}{N} \sum_{t=1}^N \varepsilon(t) \varepsilon^T(t) \quad (13)$$

which is a generalization of (5).

Several strong theorems have also been stated about the multivariable case, e.g. see Åström et al [30], Mehra [36], Woo [38], Caines [39], Ljung [40] and Mehra et al [41].

### C. A Vector Difference Equation Approach.

In order to find alternative models for the reactor also a vector difference approach was tried. Simplifying assumptions of the noise are made in order to identify the vector difference equation row by row. The noise assumptions are only adequate if there are weak couplings between the outputs considered.

The structure of the system is generalized from (1) to

$$\begin{aligned}
 [I + A_1 q^{-1} + \dots + A_n q^{-n}]y(t) &= \\
 &= [B_1 q^{-1} + \dots + B_n q^{-n}]u(t) + \\
 &+ [I + C_1 q^{-1} + \dots + C_n q^{-n}]e(t)
 \end{aligned} \tag{14}$$

where the capital letters assign constant matrices, while  $y$ ,  $u$  and  $e$  are vectors. It is clear that there is no one-to-one correspondence between (14) and (10). The likelihood function is still (11) where the residuals are defined by

$$\begin{aligned}
 \varepsilon(t) &= [I + C_1 q^{-1} + \dots + C_n q^{-n}]^{-1} * \\
 &* \{ [I + A_1 q^{-1} + \dots + A_n q^{-n}]y(t) - \\
 &- [B_1 q^{-1} + \dots + B_n q^{-n}]u(t) \}
 \end{aligned} \tag{15}$$

If it is desired to identify the model row by row, then the loss function has to be written as a sum of  $n$  functions. This is possible if  $R$  is diagonal,

$$R = \text{diag}(\lambda_1^2, \dots, \lambda_n^2) \quad (16)$$

and each matrix  $C_i$  is diagonal as well. The assumption means, that every output of the model is disturbed by a separate noise source, independent of other noise sources. With such assumptions all the parameters of  $A_i$ ,  $B_i$  and  $C_i$  are identifiable.

The parameter estimates are not unbiased, consistent or with minimum variance as for the single output case. Still these multivariable models might indicate interesting couplings which will be shown in section VI.

#### D. Recursive Parameter Estimation.

If the unknown parameters  $\theta$  in the system (9 - 10) are time variable there is no computationally simple optimal method to track the parameters recursively. A large number of suboptimal methods therefore have been proposed, and the Extended Kalman filter is one of the simplest ones to find the parameters. The unknown parameter vector is estimated as part of an extended state vector. The algo-

rithm used here is described in detail in Olsson-Holst [42], where a literature survey of the application of suboptimal filters has been done as well.

The parameter vector  $\theta$  is assumed to be constant but driven by independent noise  $w$ ,

$$\theta(t+1) = \theta(t) + w(t) \quad (17)$$

The artificial noise covariance determines how fast the parameter can be tracked. In the use of Extended Kalman filter there is no simple way to choose the value of  $\text{cov}(w)$ . It has to be found by trial and error, and depends on the system noise as well as the variability of the parameters. It may, however, be found off-line using the ML method [32], [41] and then kept fixed in the Extended Kalman filter.

The sample covariance matrix of the residuals

$$\varepsilon(t) = y(t) - \hat{C}\hat{x}(t|t-1) - Du(t) \quad (18)$$

can be used as a test quantity to judge the quality of the results. The residuals should be a sequence of zero mean independent stochastic variables.



### E. Model Verification.

Generally the problem of verifying a model is still an art. Many different types of tests have to be performed in order to check the model behaviour. Here only the open loop behaviour of different models has been compared. It should, however, be emphasized that the final test of a model should be performed in closed loop. Then the real process should be controlled by a controller based on the achieved model. The model has also to be tested if it is really predictive. Then a model achieved from one experiment should be compared with the real output from another experiment.

Even if the parameters of two models are close to each other, their step responses might be quite different. If two models have similar Bode diagrams they could reveal quite different time behaviour. Even if the residuals are zero mean and white it does not mean that a better model cannot be found. These examples indicate, that the model verification is most important and also difficult.

As the ML method is based heavily on the residual properties, the residuals should primarily be tested for independence and normality and independence to the inputs.

The loss function changes are tested against the F-

test quantity (6) in the MISO case complemented with the Akaike test (7). The model error, defined as the difference between the real output and the output of the deterministic part of the model, is computed.

The standard deviation of the parameters has been checked. If the model order is too high, then the Fisher Information matrix becomes singular, which means that corresponding parameter estimates are linearly correlated and the parameter covariances will be very high.

The discrete models have often been transformed to continuous models in order to compare time constants and zeroes with physical knowledge. Bode plots have been calculated and simulations have been performed.

Single-input-single-output models then have been written in the transfer function form

$$G(s) = k_0 + \sum_{i=1}^{n_1} \frac{k_i}{T_i s + 1} + \sum_{j=1}^{n_2} \frac{\kappa_j \left( \frac{1}{z_j} s + 1 \right)}{\left( \frac{s}{\omega_0} \right)^2 + 2\zeta \left( \frac{s}{\omega_0} \right) + 1} \quad (19)$$

where  $n_1 + n_2$  is the order of the system.

## F. Computational Aspects.

Some practical considerations on the computations are given in this paragraph.

### 1. Data Analysis.

Before the measurement data is used for parameter estimation, several stages of preliminary data analysis are executed. The variables are plotted in order to detect outliers, trends and abnormal behaviour. The relation between inputs and outputs can be inspected and the signal to noise ratios could be visualized. Mean values are subtracted and trend corrections are made in some cases. Cross correlation analysis has also been performed in order to verify relations between the different variables.

The data preparation and analysis part of the identification work should not be underestimated. Data must be in suitable form, programs must be stream-lined and be supplied with adequate inputs and outputs.

### 2. Identification Programs.

Most of the data analysis and identifications have been performed on the Univac 1108 computer at the Lund University Data Center. The program package for MISO identification was written by Gustavsson [43]. The ML identification program for multivariable systems has been writ-

ten by Källström, see [44]. The Extended Kalman program is described in Olsson-Holst [42].

In data analysis, parameter estimation or model verification the control engineer must often check intermediate results before he can proceed to the next step of the modeling phase. It is therefore virtually impossible and not even desirable to automate all the different partial decisions and create one general model building program.

The need for interactive programs was realized a long time ago at the Department of Automatic Control at Lund Institute of Technology, and such a program system IDPAC has now been constructed to solve MISO identification and data analysis problems on an interactive basis, see Gustavsson [25], [45]. However, most of the identifications discussed in the present paper were performed before the interactive program was completed.

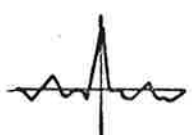
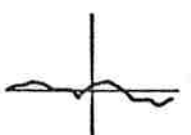
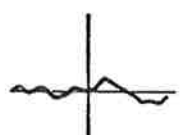

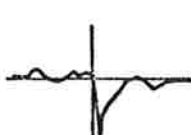

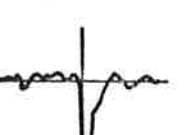

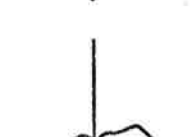
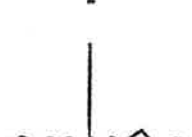
## V. MULTIPLE-INPUT-SINGLE-OUTPUT MODELS.

In this section we will consider models for four important variables of the plant, viz. the nuclear power and the primary (vessel), secondary and tertiary pressures, called C10, P13, P61 and P62 respectively in Fig. 2.

Correlation analysis between the actual inputs and outputs has been applied in order to get a more substantial information about the couplings in the plant, than was presented in section II. The actual cross correlations are drawn in table 2. Some correlations are quite clear (e.g.  $u_2 \rightarrow P62$ ) while some others are obscure ( $u_3 \rightarrow P61$ ). The ML identification gave, however, a significant relation in the latter case.

TABLE 2

Qualitative correlations between the examined inputs and outputs (max. time lag 10 min.).

Output Input	Nuclear power C10	Vessel pressure P13	Secondary pressure P61	Tertiary pressure P62
$u_1$ (VA770)				
$u_2$ (VB282)				
$u_3$ (rods)				

The interaction between the actual inputs and outputs could be qualitatively understood if Fig. 2 is considered. The influence of the different inputs were discussed in II.C. The valve  $u_1$  (VA 770) has a limited control authority but influences the nuclear power significantly. The influence on the pressures is, however, quite small. It is natural that a disturbance from  $u_1$  is successively damped out from the subcooling circuit to the core and further to the secondary and tertiary heat removal circuits. The valve  $u_2$  (VB 282) has a much higher control authority than  $u_1$  and therefore the relation to all the actual outputs are quite clear. Naturally the valve has the fastest and greatest response in the tertiary circuit but the response is damped into the secondary and primary circuits. In an analog way it is understood, that the rod ( $u_3$ ) influence on the nuclear power is significant while the influence on the primary, secondary and tertiary pressures is getting successively smaller.

#### A. Nuclear Power.

In II.B it was demonstrated that the nuclear power response on reactivity disturbances is very fast. Compared to the sampling time of 2 seconds it is prompt, which corresponds to a direct term  $b_0$  in the model (1). The valves will disturb the nuclear power through the reactivity feedbacks and consequently the dominating time constants for these loops will be longer.

### 1. Reactivity Input ( $u_3$ ).

In preliminary experiments, see [1], it was found, that the reactivity input - nuclear power output loop could be described by third or fourth order dynamics. The time constants in experiment 1 were found to be 0.7, 8.9 and about 500 seconds respectively. Typically the input PRBS sequence was very fast (see III.C) and the slow time constant has consequently been determined poorly.

Now, we consider experiments 2 and 3 where the rod reactivity input is used. In expt. 2 there is only this input, but in expt. 3 the valve  $u_2$  is also perturbed independently. Now, if the system is linear, the superposition principle should be valid. As the experimental conditions are essentially the same for experiments 2 and 3 the model parameters should be similar. Table 3 shows the parameters for model (1) with corresponding standard deviations from the Cramér-Rao inequality. The results show that at least the  $a_i$  and  $b_i$  parameters are close to each other with the differences well within one standard deviation. The  $c_i$  parameters, however, show a larger discrepancy. This is quite reasonable, as different modes have been excited in the two experiments.

It is noticed that the  $c_2$  coefficients are quite small in both cases. A model with only  $c_2 = 0$ , however, should have no clear physical interpretation. If instead  $c_3$  is

TABLE 3

Identification results relating the nuclear power to the steam valve ( $u_2$ ) and to reactivity ( $u_3$ ).

Experiment	2	3	2	3
	N=2000	N=1900		
$a_1$	$-1.662 \pm .041$	$-1.626 \pm .078$	$c_1$	$-.726 \pm .047$ $-.579 \pm .084$
$a_2$	$.713 \pm .045$	$.683 \pm .082$	$c_2$	$-.049 \pm .043$ $.025 \pm .034$
$a_3$	$-.044 \pm .016$	$-.044 \pm .017$	$c_3$	$-.063 \pm .031$ $-.054 \pm .025$
		$u_2 (*10^2)$		
$b_1$		$-.151 \pm .057$	$\lambda$	$.253 * 10^{-1}$ $.282 * 10^{-1}$
$b_2$		$.134 \pm .098$		
$b_3$		$-.098 \pm .060$	Poles	$.981; .607;$ $.966; .581$ $.074$ $.078$
	$u_3 (*10)$	$u_3 (*10)$		
$b_0$	$.236 \pm .009$	$.233 \pm .010$		
$b_1$	$.221 \pm .020$	$.232 \pm .026$		
$b_2$	$-.853 \pm .024$	$-.837 \pm .034$		
$b_3$	$.402 \pm .025$	$.386 \pm .045$		

neglected no better model could be obtained.

Now consider the continuous transfer functions corresponding to the parameters in table 3. Their coefficients (see eqn. (19)) , are listed in table 4. The term  $k_0$  corresponds to the prompt input  $b_0$  in model (1). No standard deviations are derived from the results in table 3.



TABLE 4

Continuous transfer functions of nuclear power.

Exp.	2	3	3
Input	$u_3$	$u_3$	$u_2$
$T_1$ (sec.)	0.8		0.8
$T_2$ (sec.)	4.0		3.7
$T_3$ (sec.)	104		59
$k_0*10$	0.24	0.23	0
$k_1*10$	0.76	0.78	-0.021
$k_2*10$	-0.23	-0.29	0.088
$k_3*10$	0.096	0.35	-0.95

There is found a very fast time constant of 0.8 seconds. It is clearly significant despite the sampling interval of 2 seconds. It can be explained by the actuator dynamics. Due to the sampling theorem it is still possible to detect the fast time constant. Similar experiences are reported by Gustavsson [25].

The next time constant is determined to 3.7 or 4 seconds. The fuel dynamics should have a time constant of about 8-10 seconds and the result from expt. 1 seems to

be reasonable. There are, of course, other dynamical effects added to the computed time constant, such as pressure and flow variations, which explain the smaller value. The longest time constant is determined quite poorly, especially in expt. 1. It comes from the heat removal circuit dynamics and it should be of the order one or two minutes.

As remarked before the poor accuracy is partly due to the input sequence. The longest pulse of 196 seconds is apparently not long enough, see III.C. The short sampling interval is also important. The actual discrete pole is situated close to the unit circle, see table 3. Therefore a small numerical error in the computations can create a significant change of the time constant. For example, if the pole 0.981 is changed  $\pm 0.001$  the corresponding time constant would be moved from 104 to 110 or 99 seconds respectively.

Now consider the coefficients  $k_i$  of table 4, which indicate how the different modes are amplified. First compare the rod influence on different modes. The reactivity input is most significant in the fast modes. Thus both  $k_0$  and  $k_1$  are significant and quite similar in the two experiments. Especially  $k_3$  is much larger in expt. 3. This might indicate, that the low frequencies have been more excited in expt. 3 due to the extra input from  $u_2$ . We also notice the negative sign of  $k_2$ . It shows a clear negative reactivity feedback from the fuel temperature.

## 2. Steam Valve Input ( $u_2$ ).

Table 3 shows clearly, that the  $b_i$  parameters corresponding to  $u_2$  (VB 282) are less accurate than those corresponding to  $u_3$  (rods). This is natural, as the nuclear power is perturbed more by the rods than by the valve  $u_2$ .

An attempt was made to get better model accuracy by introducing different time delays for  $u_2$ , but no improvement was obtained. The time constants are, of course, the same as for the rod input in expt. 3, but the mode amplifications are different. Table 4 shows that the low frequencies are more amplified by  $u_2$  than the high ones. The relative influence of  $u_3$  and  $u_2$  is also shown by table 4. The rod input  $u_3$  dominates in the fast modes ( $k_1$  and  $k_2$ ), while the valve dominates in the low frequency range ( $k_3$ ). The static amplification from the valve  $u_2$  to the nuclear power should be positive (see II.C). In tables 3 and 4 it is negative, and the model has no non-minimum phase behaviour. Expt. 5 gives similar results. The explanation for this discrepancy has to do with the sampling time, experiment length and input sequence. Previous step responses showed a slow non-minimum phase response (Fig. 7). It takes about two minutes for the step response to get positive after the negative undershoot. This behaviour is too slow to be detected in the experiments. Therefore the model has a negative numerator ( $k_3$  in table 4) for the slow time constant. Observe, however, that the signs of  $k_1$  and  $k_2$  are

reasonable in accordance with the discussion of II.C.

The standard deviation  $\lambda$  of the one step prediction error in table 3 is 0.025 and 0.028 MW respectively, which is close to the instrument noise level, see III.D.

A section of expt. 3 has been plotted in Fig. 8. The plots can demonstrate some features of the identification method. The nuclear power has a negative trend between 56 and 62 minutes. At about  $t = 62$  it suddenly increases again. The model, however, does not follow the slow trend and the positive change. The residuals  $\epsilon$  are large at time 62. The reason is, that an absorbtion rod was moved manually during the experiment to keep the power within permitted limits. This input could, of course, have been added to the other inputs. It was not included here in order to show, how the ML method can detect abnormal behaviour during an experiment.

### 3. Subcooling Valve Input ( $u_1$ ).

In expt. 5 the valves  $u_1$  and  $u_2$  were moved independently of each other and a corresponding model of the nuclear power was obtained. This model is also of third order. In contrast to previous models there are complex poles. The continuous transfer function is written in one real and one complex mode, according to (19). The coefficients are shown in table 5.

TABLE 5

Continuous transfer function of the  
nuclear power, expt 5.

Input	$u_1$	$u_2$
$T_1$ (sec.)	68	
$z_1$	-0.58	0.18
$\omega_0$	0.23	
$\zeta$	0.27	
$k_1 * 10^3$	1.62	-103
$\kappa_1 * 10^3$	9.8	5.2

The complex poles are lightly damped. The period time is about 28 seconds. Similar oscillations have been observed earlier when the subcooling valve has been moved, see Bjørlo et al [46]. A significant amplification of the nuclear power was achieved when the valve was exciting the system at a period of about 25 seconds.

The fast time constants which were excited by the absorption rod have not been detected here by the valves. A slow time constant of 68 seconds is found and is not too far away from what was obtained in expt. 3, where valve  $u_2$  was also perturbed.

The negative value of  $z_1$  indicates that the system is non minimum phase. Actually there are two zeroes in the

right half plane of the transfer function from  $u_1$  to the nuclear power.

### B. Primary Pressure.

Primary pressure input-output models have been studied in a similar way to those for the nuclear power. The steam valve  $u_2$  is the dominating input, and generally the pressure dynamics is much slower than the nuclear power dynamics, as the pressure has to be influenced through the heat flux (see Fig. 3). Most of the identified models are of order three or four. In most cases the fourth order models have large parameter covariances, even if the loss function is acceptable, indicating that the third order models may be adequate.

#### 1. Reactivity Input ( $u_3$ ).

The influence from  $u_3$  is much less than for the nuclear power. From experiments 1 and 2 the models obtained were quite poor, though third order models were accepted when parameter accuracy, loss function, and residual tests were considered. The parameters of expt. 2 are shown in table 6 and its continuous transform (19) in table 7.

The fast time constant related to the actuator dynamics is still statistically significant. A combination of actuator dynamics and the fuel dynamics might explain the 2 se-

cond time constant. The longest time constant is again related to the heat removal circuit dynamics.

TABLE 6

Models from different experiments relating primary (vessel) pressure to the different input signals.

Exp.	2	3	4	5
N	1000	1900	1000	1000
$a_1$	$-2.304 \pm .006$	$-2.077 \pm .007$	$-2.121 \pm .031$	$-2.155 \pm .017$
$a_2$	$1.665 \pm .011$	$1.349 \pm .012$	$1.414 \pm .058$	$1.478 \pm .031$
$a_3$	$-.361 \pm .006$	$-.269 \pm .006$	$-.291 \pm .027$	$-.321 \pm .015$
		$u_2 (*10^4)$	$u_2 (*10^4)$	$u_1 (*10^5)$
$b_1$		$-.060 \pm .014$	-	$-.159 \pm .080$
$b_2$		$-.221 \pm .025$	$-.252 \pm .010$	$-.075 \pm .140$
$b_3$		$.079 \pm .016$	-	$.390 \pm .083$
	$u_3 (*10^4)$	$u_3 (*10^4)$	$u_3 (*10^4)$	$u_2 (*10^4)$
$b_1$	$.497 \pm .017$	$.453 \pm .025$	$.092 \pm .055$	$.013 \pm .015$
$b_2$	$-.490 \pm .017$	$-.181 \pm .045$	$.467 \pm .098$	$-.229 \pm .017$
$b_3$	0	$-.180 \pm .025$	$-.498 \pm .057$	0
$c_1$	$-1.176 \pm .029$	$-.893 \pm .027$	$-.790 \pm .047$	$-.751 \pm .036$
$c_2$	$.417 \pm .047$	$.395 \pm .036$	$.328 \pm .058$	$.405 \pm .037$
$c_3$	$-.081 \pm .029$	$-.024 \pm .027$	$.032 \pm .046$	$-.031 \pm .033$
$\lambda$	$.663 * 10^{-4}$	$.724 * 10^{-4}$	$.749 * 10^{-4}$	$.753 * 10^{-4}$
Poles	$.997; .909;$ $.398$	$.983; .706;$ $.387$	$.984; .736;$ $.401$	$.987; .708;$ $.459$

TABLE 7

Continuous transfer functions relating primary pressure to the different inputs.

Exp.	2		3		4		5	
Input	$u_3$	$u_2$	$u_3$	$u_2$	$u_3$	$u_1$	$u_2$	
$T_1$ sec	2.2		2.1		2.2		2.6	
$T_2$ sec	20		5.8		6.5		5.8	
$T_3$ sec	665		119		123		157	
$k_1 \cdot 10^4$	-0.64	-0.13	-1.6	-0.87	-2.5	0.45	-1.4	
$k_2 \cdot 10^4$	8.0	4.1	3.2	8.5	4.8	-1.3	7.7	
$k_3 \cdot 10^4$	39	-71	29	-106	22	8.6	-114	

## 2. Steam Valve Input ( $u_2$ ).

Different results from experiments 3, 4 and 5 will now be compared. In all the fourth order models a negative discrete pole was found. As such a model has no continuous corresponding model it is difficult to make any physical interpretations. Therefore the third order models are discussed. The problem with negative discrete poles is considered further in paragraph E. In all models the parameter  $c_3$  is poorly determined and may be set to zero.

There is a long time constant corresponding to a pole very close to the unit circle in the discrete model. As before, this causes a poor accuracy of the long time constant, and the static amplification is also inaccurate. The fol-



lowing points should be noted:

- (i) The  $a_i$  parameters in the three experiments are quite close to each other.
- (ii) Consider the  $b_i$  parameters corresponding to  $u_2$  in table 6. Experiments 3 and 4 are compared. In expt. 4  $b_1$  and  $b_3$  were removed in order to get better parameter covariances. No significant change of the loss function was observed. Corresponding parameter  $b_1$  in experiment 5 could also have been eliminated. Now look at the  $b_i$  parameters for the reactivity input  $u_3$ . In expt. 4,  $b_1$  is much smaller than in experiments 2 and 3. There is no obvious explanation available. The elimination of  $b_1$  and  $b_3$  in expt. 4 for the input  $u_2$  changed the actual parameter a little amount. Probably the difference between the experiments has to do with the fact, that different rods were used in expt. 4 than in previous experiments.
- (iii) The parameter standard deviation depends asymptotically on  $\sqrt{N}$ , where  $N$  is the number of samples. The results in experiments 3 and 4 can be compared, and the parameter covariances roughly follow such a law.
- (iv) The time constants of about 2 and 6 seconds probably represent combinations of actuator dynamics and fuel dynamics.

(v) Fig. 9 shows a plot of the primary pressure related to the steam valve and reactivity inputs in experiment 3. The model is based on data from 40 to 72 min. and the simulation of the model is made for the time after 72 min. Observe, that the model error makes a positive jump at about  $t = 85$ . The reason is, that a control rod was moved manually. As the manual change is not included in the simulation a model error results. At the same time there is a large value in the residuals  $\epsilon$  which can be observed as a pulse in the plot.

(vi) The model error varies slowly with a period of several minutes. This indicates that there are slow time constants which are not accurately found in the model. In closed loop, however, such slow variations can be taken care of easily by the controller.

### 3. Subcooling Valve Input ( $u_3$ ).

The subcooling valve ( $u_1$ ) has been used as an input in expt. 5, and the model is shown in the tables 6 and 7. The time constants were discussed in previous section. In order to compare the influence from the different valves  $u_1$  and  $u_2$  the coefficients  $k_1$  from experiments 4 and 5 are compared in table 7. The following points should be noted:

(i) Even though the static amplification has a poor accuracy in the identification it is clear from expt. 5,

that the steam valve amplification is about 10 times larger and of different sign than that of the subcooling valve. A better determination of the static amplification must be made with larger sampling intervals and longer input pulses. The reason to use a longer sampling interval is, that the poles then are not situated so close to the unit circle. Numerical inaccuracies do not become so critical.

(ii) The oscillations which could be observed in the nuclear power as a result of subcooling valve perturbations are not observed in the primary pressure.

(iii) The standard deviation  $\lambda$  of the prediction error (see table 6) varies from  $0.66 \times 10^{-4}$  to  $0.75 \times 10^{-4}$ . It is considered satisfactory compared to the instrumentation noise level, discussed in chapter III.D.

### C. Secondary and Tertiary Pressures.

In the introduction of section V it was emphasized that the influence of the steam valve  $u_2$  is strong for the secondary and tertiary circuits. Especially the correlation to the tertiary pressure is very good. On the other hand the influences from the reactivity or the subcooling valve changes are poor or negligible.

### 1. Reactivity Input ( $u_3$ ).

Because of the poor correlation only a first order significant model was found for the secondary pressure. A time delay of 6 seconds was estimated (cf. table 2). No relation at all between  $u_3$  and the tertiary pressure was found by the ML identifications.

### 2. Steam Valve Input ( $u_2$ ).

In table 8 the identification results are shown. Consider the first column, where the secondary pressure is related to the steam valve and the reactivity. When the present model is compared with a second order model, a high test quantity (6) is achieved ( $F = 124$ ). Therefore the third order model is accepted over the second order model. The table shows that the  $b_i$  estimates corresponding to reactivity input are much more inaccurate than those for the steam valve input.

The continuous model (19) time constants are shown in table 9. The longest time constant is not very precise. The other two can be compared to corresponding results for the primary pressure, table 7. Instead of accepting the fast time constant 0.66 seconds a direct input term ( $b_0 \neq 0$  in (1)) was tried out, and a significantly better result was achieved. However, only models with negative discrete poles were found.

TABLE 8

Models from different experiments relating  
heat removal circuit pressures to different inputs.

Output	Sec. press.	Sec. press.	Tert. press.	Tert. press.
Exp.	4	5	3	3
$a_1$	$-1.877 \pm .023$	$-1.898 \pm .015$	$-1.559 \pm .012$	$-1.534 \pm .003$
$a_2$	$.918 \pm .044$	$.938 \pm .031$	$.568 \pm .011$	$.543 \pm .003$
$a_3$	$-.040 \pm .023$	$-.038 \pm .017$	-	-
	$\underline{u_2 (*10)}$	$\underline{u_1 (*10^4)}$	$\underline{u_2 (*100)}$	$\underline{u_2 (*100)}$
$b_0$	-	-	-	$-.039 \pm .0003$
$b_1$	$-.115 \pm .005$	$.574 \pm .168$	$-.129 \pm .003$	$-.077 \pm .0006$
$b_2$	$-.087 \pm .012$	-	$.120 \pm .003$	$.103 \pm .0004$
$b_3$	$.173 \pm .009$	-	-	-
	$\underline{u_3 (*100)}$	$\underline{u_2 (*10)}$		
$b_1$	$-.170 \pm .131$	$-.109 \pm .004$		
$b_2$	$.388 \pm .252$	$-.075 \pm .010$		
$b_3$	$-.183 \pm .135$	$.163 \pm .006$		
$c_1$	$-1.323 \pm .043$	$-1.256 \pm .021$	$-.385 \pm .073$	$.434 \pm .028$
$c_2$	$.575 \pm .082$	$.450 \pm .028$	$-.030 \pm .047$	$.089 \pm .026$
$c_3$	$-.076 \pm .054$	$-.023 \pm .023$	-	-
$\lambda$	$.194 \cdot 10^{-3}$	$.188 \cdot 10^{-3}$	$.478 \cdot 10^{-3}$	$.174 \cdot 10^{-3}$
$V$			2.171	.2873
Poles	.986; .843;	.989; .865; ,	.979; .580	.977; .556
	.048	.044		

TABLE 9

Continuous transfer functions relating secondary and tertiary pressures to the different inputs.

Output	Sec. press.	Sec. press.	Tert. press.	Tert. press.
Expt.	4	5	3	3
$T_1$ (sec)	0.7	0.6	3.7	3.4
$T_2$ (sec)	11.7	13.8	126	98
$T_3$ (sec)	138	178	-	-
	$u_2 (*10^3)$	$u_2 (*10^3)$	$u_2 (*10^4)$	$u_2 (*10^4)$
$k_0$	-	-	-	-0.039
$k_1$	0.24	0.22	-0.27	-0.25
$k_2$	-1.02	-1.21	-1.37	-1.15
$k_3$	-12.6	-13.6	-	-
	$u_3 (*10^3)$	$u_1 (*10^6)$		
$k_1$	-0.023	0.0015		
$k_2$	-0.131	-31.6		
$k_3$	1.79	430		

For the tertiary pressure it is natural to expect the fastest time constant to be even smaller. In fact, this time constant is too small to be estimated with the actual sampling time and a second order model is found with the shortest time constant 3.7 seconds (tables 8 and 9, third columns). A closer examination of Fig. 6 will also reveal

one long and one short time constant for the tertiary pressure. By adding a direct input term  $b_0$  an exceptional improvement of the loss function is found, corresponding to an F test quantity of 8124 (column 4 in tables 8 and 9). Also the parameter accuracy is improved. A significant improvement of the loss function can be achieved for third order models, but negative discrete poles or pole - zero cancellation appears. The time constants for the tertiary pressure are smaller than for the secondary pressure, which is natural (see table 9).

Fig. 10 shows a plot of the secondary pressure in expt. 3, related to steam valve and reactivity. The model is based on an observation record from 40 - 72 min. in the experiment and is used to predict from 80 to 94 min. The residuals have a distinct spike at about 84 min. and the model error makes a positive change. The reason is the same as for the primary pressure, Fig. 9. The tertiary pressure from expt. 3 is plotted in Fig. 11. It is based on 1900 data and simulated on the same data set. The plot shows the same part of the experiment as Fig. 8. The manual movement of a rod is revealed also here by the model error change at about 62 min.

### 3. Subcooling Valve Input ( $u_1$ ).

The correlation between  $u_1$  and the secondary and tertiary pressures is poor, which has been discussed before. A significant ML model was, however, found for the secondary

pressure, and the parameters are shown in tables 8 and 9 column 2.

The standard deviation of the one step prediction error is larger than for the primary pressure (cf. tables 6 and 8) but is still considered satisfactory with respect to the instrumentation noise.

#### D. The Problem of Negative Real Discrete Poles.

In several models, especially those of high order (third or fourth) negative real poles of the discrete model have appeared. Since these models have no continuous analog they cannot be given physical interpretations. Still they may be useful for time discrete regulators. The following reasons may be given for negative discrete poles:

(i) The negative pole may reflect that the order is too high. Generally there is a corresponding zero close to the pole in the  $C^*$  or in the  $B^*$  polynomial, but not always in both. Cancellation may be possible. In the reactor models cancellation between the  $A^*$  and  $C^*$  have been the most common case. The noise thus can be represented by a lower order transfer function, a fact which has been observed in many practical situations by e.g. Bohlin [47]. Söderström [48] has also analyzed cancellation problems.



(ii) Quantization error may cause negative discrete poles as pointed out by Åström [49]. For the secondary pressure and to a lesser extent for the primary pressure, negative poles were quite common. The quantization error of the 11 bit converter for the pressures is at least  $0.8 \cdot 10^{-4}$  normalized units. The standard deviation of the one step predictor error is  $0.7 \cdot 10^{-4}$  for the primary and  $1.9 \cdot 10^{-4}$  for the secondary pressure. Thus the quantization error cannot be neglected in comparison with the residuals. As the nuclear power one step prediction errors have been about 0.025 MW in comparison with the quantization error 0.005 MW (see III.D) this quantization error is not so serious, even though only the total power is measured.

(iii) For the secondary pressure models of second order two minima of the loss function appeared in expts. 3 and 4. The models have about the same loss function. In one model there is one negative real pole, in the other both the poles are positive real. This problem of non-uniqueness of the ML estimates has been analyzed by Söderström [50]. Similar results can also be found for the nuclear power related to the reactivity input.

## VI. VECTOR DIFFERENCE EQUATIONS.

In preceeding MISO models the couplings between the outputs or state variables of the plant have been neglected. In order to take the couplings between the inputs and outputs into account the vector difference approach, described in IV.C, was tried out. The results then are compared with the MISO models.

From a computational point of view this approach is also a MISO identification, as one row at a time of the vector difference equation is identified. Then the other outputs are used as auxiliary variables. Apart from the noise approximation there is also another error source as the different "inputs" are not independent of each other. This will also be discussed.

### A. Correlation Analysis.

In table 2 the correlation between the "real" inputs and the actual outputs is shown. Here also other pairs of inputs and outputs have been studied to find out the significant causality relations. The input has been whitened and corresponding impulse response has been estimated using Fast Fourier Transform technique. Generally 2000 data points were used.

TABLE 10

Qualitative correlations between some selected variables.

	P13	P61	P62
Nuclear power C10	-	-?	0
Vessel pressure P13		++	+
Secondary pressure P61			++
Tertiary pressure P62			

The correlation results are shown in table 10. The signs indicate a positive or negative correlation between the variables. Two signs means a clear cross correlation, one sign a low signal to noise ratio, a question mark a poor correlation while a zero means insignificant correlation.

#### B. Maximum Likelihood (ML) Identifications.

Some specific results from expt. 3 will now be discussed in order to demonstrate the model characteristics when couplings are taken into account.

Table 3 shows, that the best possible model with nuclear power (C10) as function of  $u_2$  and  $u_3$  is characterized by 13 parameters (plus 3 initial conditions), i.e. 16 parameters which give  $\lambda = 0.0282$ . If the vessel pressure (P13) is added to the model, it can be improved significantly. A

second order model - now with three inputs - corresponds to 13 parameters and  $\lambda = 0.0282$ . Significant improvements of the loss function is obtained for a third order model (19 parameters) with  $\lambda = 0.0277$  ( $F = 6$ ). Without the primary pressure as an auxiliary input no improvement is found when the number of parameters is increased to more than 13. The correlation analysis indicated that the secondary and tertiary pressures are not coupled to the nuclear power. It is verified by the ML identification, as no improvement is obtained by adding those variables as auxiliary inputs.

The plot of the model output in Fig. 12 shows an interesting behaviour compared to the previous model output, Fig. 8. The new model can follow the drift of the nuclear power between 56 and 62 minutes much better. During this time the input  $u_2$  is negative most of the time, and consequently the pressures are forced to rise, which in turn decreases the nuclear power. Thus the drift of the nuclear power is noticed through the vessel pressure P13, and the model error change at  $t \approx 62$  is consequently not so distinct. Even if the loss function is significantly smaller for the new model, the residuals in the two models look similar to each other. In principle there is only a slight scaling of the residuals. The autocovariance does not change much.

The improvement is emphasized also for the vessel

pressure. The smallest loss function for the vessel pressure related to  $u_2$  and  $u_3$  in expt. 3 was obtained for order four and 20 parameters (cf. table 6). It corresponds to  $\lambda = 0.714 \cdot 10^{-4}$ . If the nuclear power and secondary pressure are added, a third order model with 21 parameters gives  $\lambda = 0.633 \cdot 10^{-4}$ . A comparison between those models corresponds to an F test quantity (6) of 270 (1000 data). It is quite reasonable, that the vessel pressure model can be significantly improved by including other process variables. The gains from both the rods and the steam valve to the vessel pressure are quite small. According to Fig. 3 a reactivity change is first noticed in the nuclear power before it propagates to the vessel pressure. Therefore the knowledge of the nuclear power together with the reactivity input significantly increases the information about the vessel pressure. Likewise, a change in the steam flow valve causes pressure changes in the heat removal circuits which propagate towards the reactor vessel. Of similar reasons as above, the knowledge of not only the steam valve input but also the secondary pressure "input" gives a better determination of the vessel pressure.

The tertiary pressure will also be discussed. The ML identification gave significant models with both the steam valve  $u_2$  and the secondary pressure as inputs. According to table 8 (col. 4) the best model with only  $u_2$  as input has 9 parameters (including initial conditions) and  $\lambda = 0.174 \cdot 10^{-3}$ .

If the nuclear power and secondary pressure are added, a third order model with 21 parameters gives  $\lambda = 0.633 \cdot 10^{-4}$ . A comparison between those models corresponds to an F test quantity (7) of 270 (1000 data). It is quite reasonable, that the vessel pressure model can be significantly improved by including other process variables. The gains from both the rods and the steam valve to the vessel pressure are quite small. According to Fig. 3 a reactivity change is first noticed in the nuclear power before it propagates to the vessel pressure. Therefore the knowledge of the nuclear power together with reactivity input significantly increases the information about the vessel pressure. Likewise, a change in the steam flow valve causes pressure changes in the heat removal circuits which propagate towards the reactor vessel. Of similar reasons as above, the knowledge of not only the steam valve input but also the secondary pressure "input" gives a better determination of the vessel pressure.

The tertiary pressure will also be discussed. The ML identification gave significant models with both the steam valve  $u_2$  and the secondary pressure as inputs. According to table 10 the best model with only  $u_2$  as input has 9 parameters (including initial conditions) and  $\lambda = 0.174 \cdot 10^{-3}$ . With P61 added to the model a second order model with 12 parameters is accepted as the best one with  $\lambda = 0.156 \cdot 10^{-3}$ , corresponding to an F test quantity (6) of

155. No correlation was found earlier between  $u_1$ ,  $u_3$  and the tertiary pressure. The primary and secondary pressures are then links from the core dynamics to the tertiary pressure P62. The correlation analysis showed that P62 should be related also to the vessel pressure, but the ML identifications did not reveal such a relationship. The reason is, that the primary and secondary pressures are strongly correlated, so all causality relations from primary to tertiary pressures can be explained by the secondary pressure alone.

Now compare the plots in Figs. 11 and 13. The model error is significantly reduced. As for the nuclear power, the residual amplitudes are decreased but the two realizations and their covariances are quite similar.

### C. Simulations.

The whole vector difference equation (VDE) with the two inputs  $u_2$  and  $u_3$  and the four outputs can now be written in the form (14). The model contains three  $A_i$  matrices, four  $B_i$  matrices and three  $C_i$  matrices. The deterministic part of the model contains 47 parameters, 28 in the  $A_i$  matrices and 19 in the  $B_i$  matrices. The diagonal  $C_i$  matrices contain 10 parameters.

The different assumptions of the noise (see III.C)

and the inputs are tested by simulation of the VDE. When each row of the VDE was simulated separately, as in Figs. 12 and 13, then all the auxiliary variables had their observed values. When the whole VDE is simulated, then only the true inputs  $u_2$ ,  $u_3$  have their observed values given. It is natural, that the output error then is larger. Because of the new relations found, the model error is, however, still smaller than for the MISO models, as in Figs. 8 - 11. In Figs. 14 and 15 the nuclear power and the tertiary pressure are plotted from the VDE simulation made for inputs from expt. 3. Figs. 14 and 15 should be compared to the Figs. 8, 12 and 11, 13 respectively.

It is demonstrated that the VDE model output error is (in mean square) between the results of MISO identification and row-by-row VDE identification. Observe, however, that slow variations occur quite obviously also here.

## VII. A STATE MODEL.

From a control point of view it is interesting to get an accurate and still reasonably small model of the plant. An attempt is made to formulate a state model in order to achieve better physical interpretation of the model parameters. In this section a model is identified from expt. 4 using only two inputs  $u_2$  and  $u_3$ . A structure of



the plant model is derived first and the essential approximations are accounted for. Then the identification results are presented and discussed.

#### A. Derivation of a Model Structure.

In section II the qualitative behaviour of the plant was discussed, and by identification some of the most essential relations were confirmed. Here an attempt is made to quantify the assumptions of physical couplings between the different process variables. The goal is to find a linear state variable description.

It is assumed, that the variations are small, so that the nonlinear effects are negligible. The state variables are defined as deviations from stationary values.

##### 1. Kinetics.

The neutron level  $n^*$  is proportional to the nuclear power  $C_{10}$ . If one group of delayed neutrons is assumed the neutron density equation is

$$\frac{dn^*}{dt} = \frac{\delta k - \beta}{\ell} \cdot n^* + \lambda c \quad (20)$$

where  $n^*$  is the neutron density,  $c$  the concentration of delayed neutrons,  $\beta$  the delayed neutron fraction,  $\lambda$  a

weighted average value of the decay constants of the precursors of the six groups of delayed neutrons,  $\ell$  the neutron generation time and  $\delta k = k_{\text{eff}} - 1 \approx \text{reactivity}$ . The last term is discussed in paragraph 6.

The one group description of delayed neutrons is

$$\frac{dc}{dt} = \frac{\beta}{\ell} n^* - \lambda c \quad (21)$$

As the neutron kinetics is very fast compared to other phenomena in the plant a prompt jump approximation is made, i.e.  $dn^*/dt$  is put to zero. This makes the nuclear power an algebraic equation of the other state variables, according to (20).

## 2. Fuel Temperature Dynamics.

The heat content of the fuel elements is represented by the average fuel temperature  $\theta_f$ . As it is influenced by heat transfer through the fission and is decreased by the coolant, the following dynamics

$$T_f \frac{d\theta_f}{dt} = -\theta_f + \gamma_1 n^* + \gamma_2 \theta_c \quad (22)$$

is assumed, where  $\gamma_i$  are constants and  $T_f$  is an average time constant for the fuel elements determined by their total heat capacity. It is initially assumed to be 8 se-

conds. The coolant temperature  $\theta_c$  will later be represented by an average water temperature  $\theta_w$  and the coefficient  $\gamma_2$  is found to be close to zero.

### 3. Coolant and Moderator Dynamics.

The hydraulics, coolant and moderator dynamics are probably the most complex features of the plant. Here several crucial approximations are made. All the water content in the core is represented by an average water temperature  $\theta_w$ , which then (together with fuel temperature) represents the heat flux in the core. The void content is strongly related to both heat flux and vessel pressure, and therefore it is here involved in those state variables.

The vessel pressure  $p_1$  gives, of course, no information about the void distribution along the coolant channels. The reactivity feedback from void depends not only on the average void but also on the spatial distribution of the void. Moreover the boiling boundary is not taken into account, and it is a critical variable.

It has been demonstrated in section II that the subcooled flow temperature ( $\Delta T_8$ ) is related to both the water temperature  $\theta_w$  and to the reactivity. This dynamics has not been included in the present state model, as the valve  $u_1$  was not moved in the selected experiment. The temperature changes therefore were not significant.

The structure of the water temperature equation can now be formulated. Because of the large water mass the heat capacity is large, and corresponding time constant is of the order minutes. Initially it is assumed to be 100 seconds.

The heat flux which can change the water temperature can be represented by the three states, fuel temperature, subcooled water temperature and the heat transfer through the steam transformer. Part of the heat is also due to the fact that all the fission power is not captured in the fuel, but in the moderator. The coupling to the subcooled water has been neglected. The heat flux through the steam transformer is for the moment represented by the term  $q_1$ . Then the water equation is formulated as

$$T_w \frac{d\theta_w}{dt} = -\theta_w + \gamma_3 \theta_f + \gamma_4 q_1 \quad (23)$$

#### 4. Vessel Pressure Dynamics.

According to the assumptions about the coolant the pressure must reflect many different features. This means, that the equation parameters are combinations of many physical phenomena and it is therefore very difficult to make any theoretical derivation of their numerical values.

The vessel pressure is certainly related to the heat

flux from the fuel elements and the water temperature. To a very small extent it is related to the subcooled temperature. No identification has verified any significant relation. In any case the influence from the subcooled temperature is neglected in the present experiment.

The vessel pressure also depends on the steam removal through the steam transformer to the secondary circuit. If this energy flux is represented as before by  $q_1$  the pressure equation structure is

$$\frac{dp_1}{dt} = \gamma_5 p_1 + \gamma_6 \theta_f + \gamma_7 \theta_w + \gamma_8 q_1 \quad (24)$$

### 5. Heat Removal Circuit Dynamics.

The dynamical coupling between the reactor core and the steam circuits is through the vessel pressure and the primary steam flow. As remarked before there is also a weak coupling to the water circuits through the subcooler A. The subcooling temperature and flow then can represent the essential variables for this coupling.

The heat transfer in the steam transformers and in the subcoolers now is considered. The functional difference between the steam transformers and the subcoolers is, that the latter ones have one phase flow (water) both in the primary

and in the secondary circuits. In order to simplify the model as much as possible only the steam phase is considered. It is known, that the water is only slightly subcooled in the circuits. Variations in the subcooling are considered as stochastic disturbances to the pressures.

The mass and energy balance equations for the heat exchangers have been formulated earlier by Euroola [24]. As the steam is close to saturation it is reasonable - as remarked in section II - that the temperature variations are assumed proportional to the pressure variations. Therefore the pressure is used to represent the enthalpy.

The primary steam flow variations ( $F_{41}$ ) are not negligible, as soon as the steam valve  $u_2$  has been moved. Identifications have shown that it is also significantly related to the primary pressure and to some extent to the nuclear power. Therefore we assume here that the enthalpy on the primary side of the steam transformer is described only by the vessel pressure. In section II.C it is indicated that the temperature variations on the secondary side are small. Therefore the secondary side enthalpy is also represented just by the pressure. The consequence of these arguments is, that the energy term  $q_1$  in eqs. (23) and (24) can be replaced by the secondary pressure  $p_2$ . With similar arguments the tertiary circuit dynamics is described by only one state variable, the tertiary pressure  $p_3$ .

The secondary pressure dynamics is consequently assumed to be

$$\tau_2 \frac{dp_2}{dt} = q_{12} - q_{23} \quad (25)$$

where  $q_{12}$  and  $q_{23}$  are the heat fluxes from the primary to secondary and from secondary to tertiary circuits respectively. The heat fluxes are assumed to be related to the pressures in the following way:

$$q_{12} = v_1 p_1 - v_2 p_2$$

$$q_{23} = v_3 p_2 - v_4 p_3$$

where  $v_i$  are constants. This results in

$$\frac{dp_2}{dt} = \gamma_9 p_1 + \gamma_{10} p_2 + \gamma_{11} p_3 \quad (26)$$

For the tertiary system we have

$$\tau_3 \frac{dp_3}{dt} = q_{23} - q_3 \quad (27)$$

where  $q_3$  is the heat removed from the tertiary system.

We assume

$$q_3 = v_5 p_3 + v_6 u_2$$

The state equation then is

$$\frac{dp_3}{dt} = \gamma_{12} p_2 + \gamma_{13} p_3 + \gamma_{14} u_2 \quad (28)$$

#### 6. Reactivity Feedbacks.

The reactivity term  $\delta k$  in eq. (20) defines the coupling between the kinetic equations and the rest of the plant. The feedback effects have been indicated in Fig. 3. The void content has been represented by vessel pressure and by water temperature. As the steam removal influences the void content we also include the secondary pressure among the reactivity feedbacks. It is assumed that a linear relation holds,

$$\delta k = u_3 + \gamma_{15} \theta_f + \gamma_{16} \theta_w + \gamma_{17} p_1 + \gamma_{18} p_2 \quad (29)$$

where  $u_3$  represents the net reactivity from the rods. The feedback from the subcooled water is neglected.



## 7. Summary

To summarize the structure, the state vector of the linear model is defined as

- $x_1$  delayed neutrons  $c$  (21)
- $x_2$  fuel temperature  $\theta_f$  (22)
- $x_3$  water temperature  $\theta_w$  (23)
- $x_4$  vessel pressure  $p_1$  (24)
- $x_5$  secondary pressure  $p_2$  (26)
- $x_6$  tertiary pressure  $p_3$  (28)

The input vector has only the two inputs steam valve and reactivity.

The model is described by

$$\frac{dx}{dt} = Ax + Bu \quad (30)$$

$$A = \begin{bmatrix} 0 & \underline{a_{12}} & \underline{a_{13}} & \underline{a_{14}} & \underline{a_{15}} & 0 \\ \underline{a_{21}} & \underline{a_{22}} & \underline{a_{23}} & \underline{a_{24}} & \underline{a_{25}} & 0 \\ 0 & \underline{a_{32}} & \underline{a_{33}} & \underline{a_{34}} & \underline{a_{35}} & 0 \\ 0 & \underline{a_{42}} & \underline{a_{43}} & \underline{a_{44}} & \underline{a_{45}} & 0 \\ 0 & 0 & 0 & \underline{a_{54}} & \underline{a_{55}} & \underline{a_{56}} \\ 0 & 0 & 0 & 0 & \underline{a_{65}} & \underline{a_{66}} \end{bmatrix} \quad B = \begin{bmatrix} 0 & \underline{b_{12}} \\ 0 & \underline{b_{22}} \\ 0 & 0 \\ 0 & 0 \\ 0 & 0 \\ \underline{b_{61}} & 0 \end{bmatrix} \quad (31)$$

The underlined elements will be discussed in section VIII.

The three pressures  $p_1 - p_3$  are measured, but the nuclear power has not been used as an output. The general form of the nuclear power related to the other state variables is derived from (20) and (29) but the parameters are unknown. In order to limit the complexity of unknown parameters the nuclear power measurements therefore are not used.

The output equation then is

$$y = Cx$$

where

$$C = \begin{pmatrix} 0 & 0 & 0 & 1 & 0 & 0 \\ 0 & 0 & 0 & 0 & 1 & 0 \\ 0 & 0 & 0 & 0 & 0 & 1 \end{pmatrix} \quad (32)$$

#### B. Parameter Identification.

The identification of the state model is now presented. First the noise is discussed.

### 1. Noise Description.

In III.D the instrument noise is considered and is found to be quite small. Thus the major contribution to the residuals are due to process noise and model errors.

There are many noise sources in the plant, a fact which is demonstrated by the MISO identifications. The boiling is a large noise source term, which affects  $x_4$ . Temperature variations in coolant, subcooled water affect  $x_3$ . The saturation temperature is changed due to heat flux variations. Varying degrees of subcooling in the water phase in the heat removal circuits will disturb the pressures  $x_5$  and  $x_6$ . Also the flow variations in the circuits create disturbances.

The process noise terms also can represent modeling errors to some extent.

### 2. Identification Results.

The stochastic structure of the system is described by eqs. (8) - (9). From expt. 4 a sequence of 800 samples have been used.

In the first approach the matrices  $K$  and  $D$  of (10) were assumed to be zero. With 8 parameters assumed unknown in the  $A$  and  $B$  matrices a minimum point was found corresponding to

$$\text{tr}(\hat{R}) = 0.123 \cdot 10^{-3}$$

(see (13)). This corresponds to standard deviations of the prediction errors  $0.50 \cdot 10^{-2}$  (vessel pressure),  $0.74 \cdot 10^{-2}$  (secondary pressure) and  $0.66 \cdot 10^{-2}$  (tertiary pressure). These errors are very large compared to previous MISO results ( $0.7 \cdot 10^{-4}$ ,  $0.19 \cdot 10^{-3}$ ,  $0.17 \cdot 10^{-3}$  respectively). Moreover, the residuals were not accepted to be white noise.

It is clear, that process noise must be included. First only three non-zero elements of the K matrix were tried,  $k_{41}$ ,  $k_{52}$  and  $k_{63}$ .

In order to limit the computations not more than 15 parameters at a time were assumed to be unknown in the A, B and K matrices. With K included a significant improvement was obtained. The loss function decreased noticeably. The standard deviations of the prediction errors for the three pressures were  $0.88 \cdot 10^{-3}$ ,  $0.96 \cdot 10^{-3}$  and  $0.15 \cdot 10^{-2}$  respectively. Those values are still too large compared to the MISO results.

It is demonstrated that it is not trivial to find a correct structure in state form. Several improvements can be made, and work is in progress to improve the model

structure. It is clear, that the number of parameters in the A and B matrices (31) can be increased. In the VDE approach not less than 34 significant parameters were found in the deterministic part of the model relating two inputs to the three selected output pressures. In the state equation identification the number of degrees of freedom (equal to the number of parameters to be identified) for fitting the observed data has been reduced. In A and B (31) there are only 25 parameters. Clearly the number of states should be increased. The assumptions about the core dynamics have to be more elaborate. One variable describing the void content and two different states for the coolant and moderator temperature would be a significant improvement. Moreover, previous identifications showed, that the primary steam flow probably should be considered a separate state variable. It is also clear, that one state for each heat removal circuit is too little. The present state model has no time constant smaller than 6 seconds, and the results in V.C. clearly demonstrated that fast modes are important. Thus additional states are needed to describe the secondary and tertiary pressures better.

It is difficult to find good initial values of the K matrix, as they do not have any intuitive physical interpretation. It is maybe easier to guess parameters in the process noise covariance matrix, and then transform to K by using a Riccati equation [44].

The computational work is by no means trivial. The likelihood function is minimized numerically. The gradients are computed numerically using finite differences, and a Fletcher-Powell algorithm is used for minimization. Manual interaction has to be done to a large extent during the minimization. The intermediate results have to be judged if they are reasonable. Otherwise it is easy to get unreasonable computational times, depending on too slow convergence, wrong step lengths etc.

In Fig. 16 the first part of expt. 4 is plotted. The best model hitherto is compared to the real output values.

#### VIII. RECURSIVE IDENTIFICATION.

In expt. 7 the operating level is changed significantly by means of the subcooling. A time variable linear model could describe this phenomenon. Here an Extended Kalman filter has been applied in order to recursively track the varying parameters.

### A. Influence of Subcooling Power.

The general nature of the subcooling effects were discussed in section II.A and C. The quantitative influence of varying subcooling power has been studied by comparing experiments 6 (table 1) and 4. It was found, that not all the parameters in the A matrix (31) changed, except mainly the underlined ones.

Generally a lower subcooling power means a lesser degree of stability. Mainly the reactivity feedback coefficients (Fig. 3) will be affected. As they are hidden in the system equation coefficients a couple of examples are given here.

As soon as the subcooling power decreases there is a higher probability for boiling in the moderator. The total void content increases. The sensitivity to pressure changes will then rise and the vessel pressure influence on reactivity will grow. With a prompt jump approximation this means that  $x_1$  and  $x_2$  are primarily influenced, i.e. the parameters  $a_{14}$  and  $a_{24}$  (31). As an example  $a_{14} = -0.24$  from expt 4 with 1.95 MW subcooling, and  $a_{14} = -0.64$  at expt 6 with 1.1 MW subcooling.

In experiment 7 the subcooling power was changed manually from 1.95 to 1.4 MW during 15 minutes, while  $u_2$  and

$u_3$  were disturbed (table 1). The subcooling power is shown in Fig. 17 (upper fig.). It was not included in the model but considered as an external disturbance source. The initial condition for expt. 7 is the same as the operating level of expt. 4. Therefore the model described in VII.B is used as the starting model for the recursive parameter estimation.

### B. Parameter Tracking.

The observed variables from expt. 7 were put into an Extended Kalman filter (see IV.D) and the six time-varying parameters were tracked. There is no way to find optimal estimates of time-variable parameters in a multivariable system. It is known, that the Extended Kalman filter most often gives unreliable confidence limits on the parameter estimates. Several compensations for this have been proposed [42]. Here, however, the main interest has been to test the simplest possible filter to track the parameters.

The six unknown parameters were described as eq. (17) with an artificial noise  $w$ . Initially the covariance matrix of  $w$  was chosen diagonal, and only trial and error methods were used to find suitable values. It was found that the diagonal elements of  $\text{cov}(w)$  should lie between  $10^{-6}$  and  $10^{-7}$ , i.e. somewhat smaller than the process noise covariance elements. This is reasonable, as the



parameters are assumed to vary slowly compared to the state variables. With too small values of  $\text{cov}(w)$  the tracking was too insensitive.

In Fig. 17 an example is shown. Six parameters were estimated simultaneously and  $a_{14}$ , discussed above, is displayed. The parameter is approaching  $-0.4$  which seems to be a plausible result, as the subcooling reaches  $1.4$  MW.

It is natural to try to minimize the number of time variable parameters, as the computing time grows very fast with the size of the extended state vector. Attempts with only two time-variable parameters were not successful, but three parameters could be reasonably accurate.

The computing time for the Extended Kalman filter may be a severe constraint on an on-line computer. Here the extended state vector consists of 12 states which means a considerable computational burden. Probably even more state variables should be included in order to improve the model. Therefore it is crucial to simplify the calculations as much as possible and a tailor made filter has to be defined.

## ACKNOWLEDGEMENTS.

This work has been partially supported by the Swedish Board for Technical Development. The research has been performed in cooperation with the OECD Halden Reactor Project. The author is especially indebted to Dr. R. Grumbach, Mr. H. Roggenbauer and Mr. R. Karlsson (now with Atomenergi AB, Sweden) with the Halden Reactor Project for their participation and interest. The permission of the Project to publish the results is also gratefully acknowledged.

The team work at the Department of Automatic Control has been most valuable. Professor K.J. Åström has contributed with constructive criticism, new ideas and never failing encouraging support. Dr. I. Gustavsson has throughout the work shared his knowledge of identification and has been of invaluable help. Mr. C. Källström wrote the state model identification program. Mr. J. Holst has cooperated with the author on suboptimal filtering problems. Dr. B. Wittenmark has contributed with valuable comments and corrections when reading the manuscript. Mrs. G. Christensen has typed the manuscript and Miss B.M. Carlsson has prepared the figures.

## REFERENCES.

- [1] G. Olsson: Maximum Likelihood Identification of some Loops of the Halden Boiling Water Reactor, Report 7207, Department of Automatic Control, Lund Institute of Technology, Lund, 1972.
- [2] H. Roggenbauer, W. Seifritz, and G. Olsson: Identification and Adjoint Problems of Process Computer Control, Enlarged Halden Programme Group Meeting, Loen, Norway, 1972.
- [3] G. Olsson: Modeling and Identification of Nuclear Power Reactor Dynamics from Multivariable Experiments, Proc. 3rd IFAC Symp. on Identification and System Parameter Estimation, the Hague, the Netherlands, 1973.
- [4] I. Gustavsson: Comparison of Different Methods for Identification of Linear Models for Industrial Processes, Automatica, 1972, Vol. 8, pp. 127-142.
- [5] A.P. Sage and G.W. Masters: Identification and Modeling of Nuclear Reactors, IEEE Trans. Nucl. Sci., 1967, NS-14, pp. 279-285.
- [6] W. Ciechanowicz and S. Bogumil: On the On-line Statistical Identification of Nuclear Power Reactor Dynamics, Nucl. Sci. Engr., 1968, Vol. 31, pp. 474-483.
- [7] L.J. Habegger and R.E. Bailey: Minimum Variance Estimation of Parameters and States in Nuclear Power Sys-

- tems, Proc. 4th IFAC Congress, Warsaw, paper 12.2, 1969.
- [8] R.L. Moore and F. Schweppe: Model Identification for Adaptive Control of Nuclear Power Plants, Automatica, 1973, Vol. 9, pp. 309-318.
  - [9] A. Brouwers: Step Perturbation Experiments with the HBWR Second Fuel Charge, OECD Halden Reactor Project, HPR-51, 1964.
  - [10] V. Tosi and F. Åkerhielm: Sinusoidal Reactivity Perturbation Experiments with the HBWR Second Fuel Charge, OECD Halden Reactor Project, HPR-49, 1964.
  - [11] Y. Fishman: Pseudorandom Reactivity Perturbation Experiments with the HBWR Second Fuel Charge, OECD Halden Reactor Project, HPR-50, 1964.
  - [12] T. Eurola: Noise Experiments with the HBWR Second Fuel Charge, OECD Halden Reactor Project, HPR-53, 1964.
  - [13] T.J. Bjørlo et al: Digital Plant Control of the Halden BWR by a Concept Based on Modern Control Theory, Nucl. Sci. Engr., 1970, Vol. 39, pp. 231-240.
  - [14] H. Roggenbauer: Real-Time Nuclear Power Plant Parameter Identification with a Process Computer, Proc. 3rd IFAC Symp. on Identification and System Parameter Estimation, the Hague, the Netherlands, 1973.

- [15] E. Jamne and J.G. Siverts: Description of the HBWR Plant, OECD Halden Reactor Project, HPR-95, 1967.
- [16] J.A. Fleck, Jr.: The Dynamic Behaviour of Boiling Water Reactors, J. Nucl. Energy, Part A, 1960, Vol. 11, pp. 114-130.
- [17] S. Glasstone and M.C. Edlund: The Elements of Nuclear Reactor Theory, Van Nostrand, Princeton, N.J., 1952.
- [18] C.D.G. King: Nuclear Power Systems, MacMillan, New York, 1964.
- [19] R.V. Meghreblan and D.K. Holmes: Reactor Analysis, McGraw-Hill, New York, 1960.
- [20] L.E. Weaver: Reactor Dynamics and Control, American Elsevier, New York, 1968.
- [21] D. Wiberg: Optimal Control of Nuclear Reactor Systems, Advances in Control Systems (C. Leondes, Ed.), Vol. 5, Academic Press, N.Y., 1967.
- [22] G. Olsson: Simplified Models of Xenon Spatial Oscillations, Atomkernenergie, 1970, Vol. 16, No. 2, pp. 91-98.
- [23] H. Vollmer and A.J.W. Anderson: Development of a Dynamic Model for Heavy Water Boiling Reactors and Its Application to the HBWR, OECD Halden Reactor Project, HPR-54, 1964.
- [24] T. Eurola: Dynamic Model of the HBWR Heat Removal Circuits, OECD Halden Reactor Project, HPR-62, 1964.

- [25] I. Gustavsson: Survey of Applications of Identification in Chemical and Physical Processes, Automatica, 1975, vol. 11, pp. 3-24.
- [26] P.A.N. Briggs, K.R. Godfrey, and P.H. Hammond: Estimation of Process Dynamic Characteristics by Correlation Methods Using Pseudo Random Signals, Proc. 1st IFAC Symp. Identification in Automatic Control Systems, Prague, 1967.
- [27] I.G. Cumming: Frequency of Input Signal in Identification, Proc. 2nd IFAC Symp. Identification and Process Parameter Estimation, Prague, 1970.
- [28] I.G. Cumming: On-line Identification for the Computer Control of a Cold Rolling Mill, Automatica, 1972, Vol. 8, pp. 531-541.
- [29] F. Pettersen: Description of System Hardware for the Main Process Computer Installation at the HBWR, OECD Halden Reactor Project, HPR-123, 1971.
- [30] K.J. Åström and P. Eykhoff: System Identification, a Survey, Automatica, 1971, Vol. 7, pp. 123-162.
- [31] P. Eykhoff: System Identification, Wiley, 1974.
- [32] R.K. Mehra and J.S. Tyler: Case Studies in Aircraft Parameter Identification, Proc. 3rd IFAC Symp. on Identification and System Parameter Estimation, the Hague, the Netherlands, 1973.

- [33] K.J. Åström and T. Bohlin: Numerical Identification of Linear Dynamic Systems from Normal Operating Records, IFAC Symp. Theory on Self-Adaptive Control Systems (P.H. Hammond, ed.), Teddington, Engl., Plenum Press, N.Y., 1965.
- [34] H. Akaike: Statistical Predictor Identification, Ann. Inst. Statist. Math., 1970, Vol. 22, No. 2, pp. 203-217.
- [35] K.J. Åström: Introduction to Stochastic Control, Academic Press, N.Y., 1970.
- [36] R.K. Mehra: Identification of Stochastic Linear Systems Using Kalman Filter Representation, AIAA Journal, 1971, Vol. 9, No. 1, pp. 28-31.
- [37] J. Eaton: Identification for Control Purposes, IEEE Winter Meeting, N.Y. 1967.
- [38] K.T. Woo: Maximum Likelihood Identification of Noisy Systems, Proc. 2nd IFAC Symp. on Identification and Process Parameter Estimation, Prague, 1970.
- [39] P.E. Caines: The Parameter Estimation of State Variable Models of Multivariable Linear Systems, Control Systems Centre Report No. 146, The Univ. of Manchester, Inst. of Sci. and Techn., April, 1971.
- [40] L. Ljung: On Consistency for Prediction Error Identification Methods, Report 7405, Dept. of Automatic Control, Lund.Inst. of Technology, Lund, 1974.

- [41] R.K. Mehra and P.S. Krishnaprasad: A Unified Approach to the Structural Estimation of Distributed Lags and Stochastic Differential Equations, Third NBER Conference on Stochastic Control and Economic Systems, Washington D.C., May, 1974.
- [42] G. Olsson and J. Holst: A Comparative Study of Suboptimal Filters for Parameter Estimation, Report 7324, Dept. of Automatic Control, Lund Inst. of Techn., Lund, 1973.
- [43] I. Gustavsson: Parametric Identification of Multiple Input, Single Output Linear Dynamical Systems, Report 6907, Dept. of Automatic Control, Lund Inst. of Techn., Lund, 1969.
- [44] K.J. Åström and C. Källström: Application of System Identification Techniques to the Determination of Ship Dynamics, Proc. 3rd IFAC Symp. on Identification and System Parameter Estimation, the Hague, the Netherlands, 1973.
- [45] I. Gustavsson, S. Selander and J. Wieslander: IDPAC User's Guide, Report 7331, Dept. of Automatic Control, Lund Inst. of Techn., Lund, 1973.
- [46] T.J. Bjørlo et al: Application of Modern Control Theory for Regulation of the Nuclear Power and the Reactor Vessel Pressure of the HBWR, OECD Halden Reactor Project, HPR-131, Halden, 1971.



- [47] T. Bohlin: On the Maximum Likelihood Method of Identification, IBM J. Res. and Dev., 1970, Vol. 14, pp. 41-51.
- [48] T. Söderström: Test of Common Factors of Identified Models. Application to the Generalized Least Squares Method, Report 7328, Dept. of Automatic Control, Lund Inst. of Techn., Lund, 1973.
- [49] K.J. Åström, private communication, 1975.
- [50] T. Söderström: On the Uniqueness of Maximum Likelihood Identification, Automatica, 1975, Vol. 11, pp. 193-197.

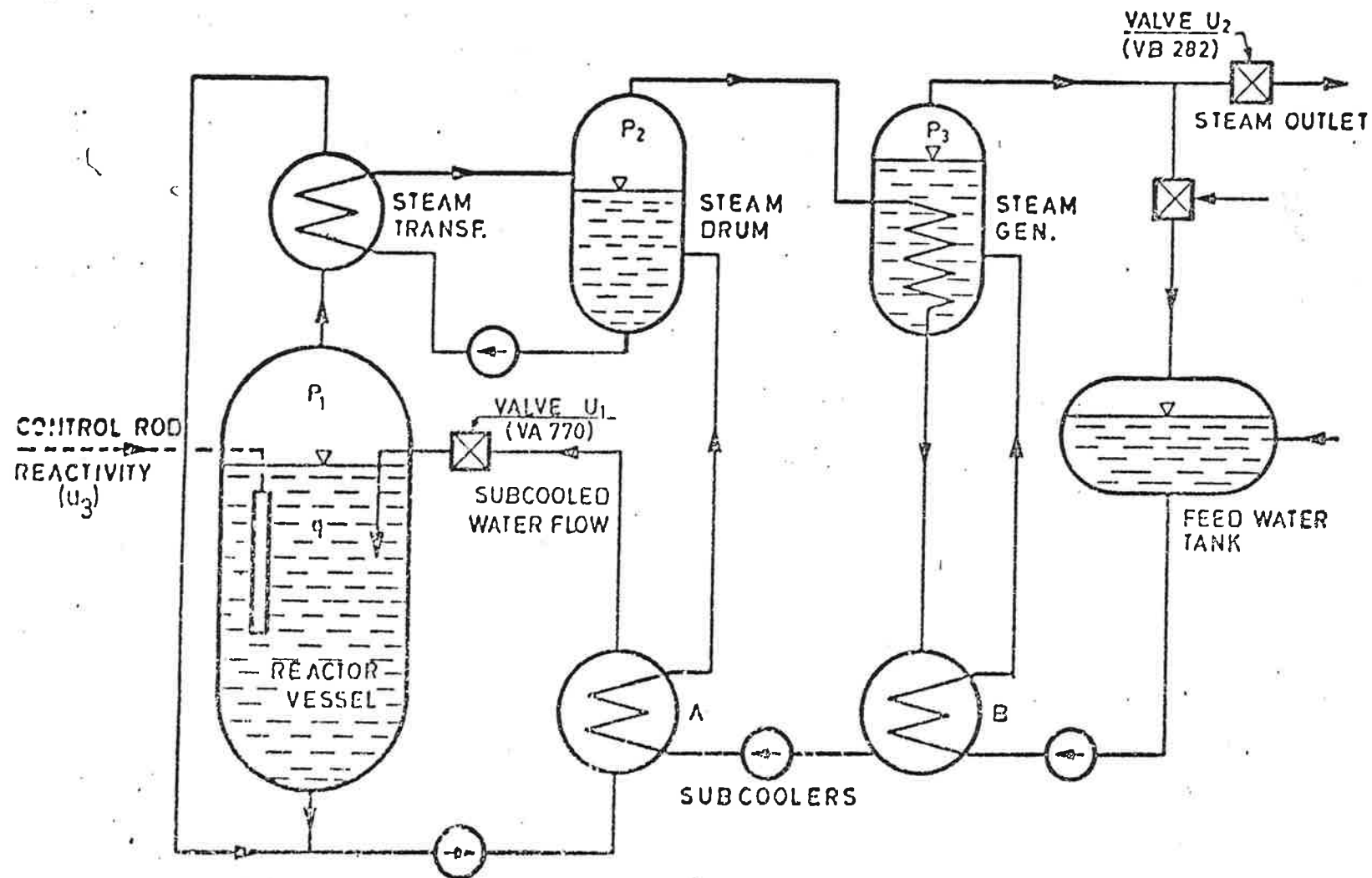


Fig. 1. Simplified flow sheet of the HBWR plant.

Reprinted by courtesy of the Halden Reactor Project.

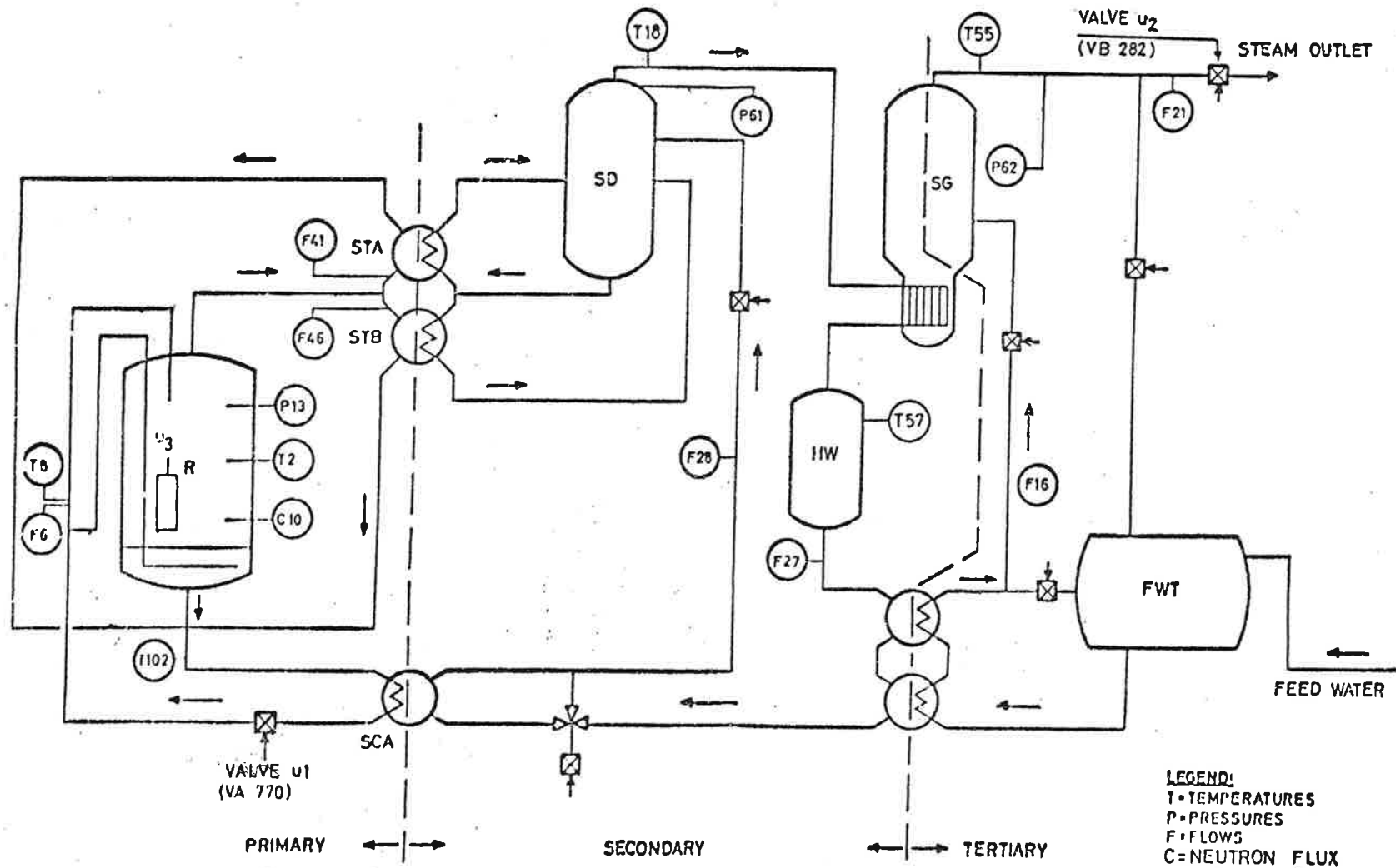


Fig. 2. Variables registered for the identifications.  
Reprinted by courtesy of the Halden Reactor Project.

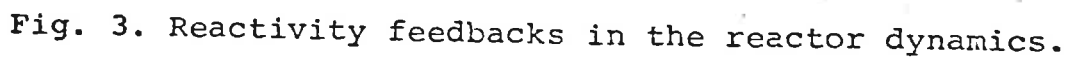


Fig. 3. Reactivity feedbacks in the reactor dynamics.

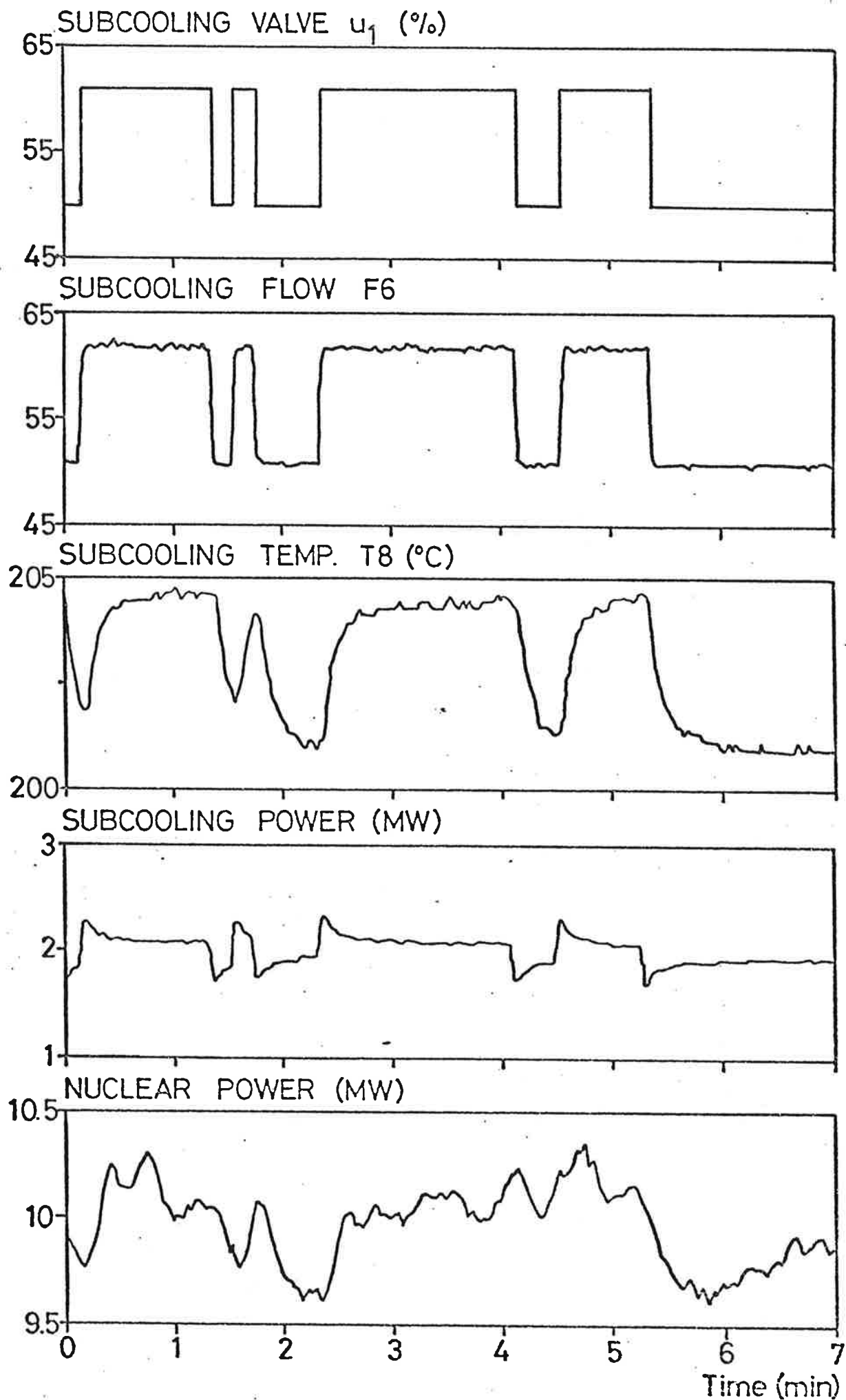


Fig. 4. Typical responses to changes in  $u_1$ .

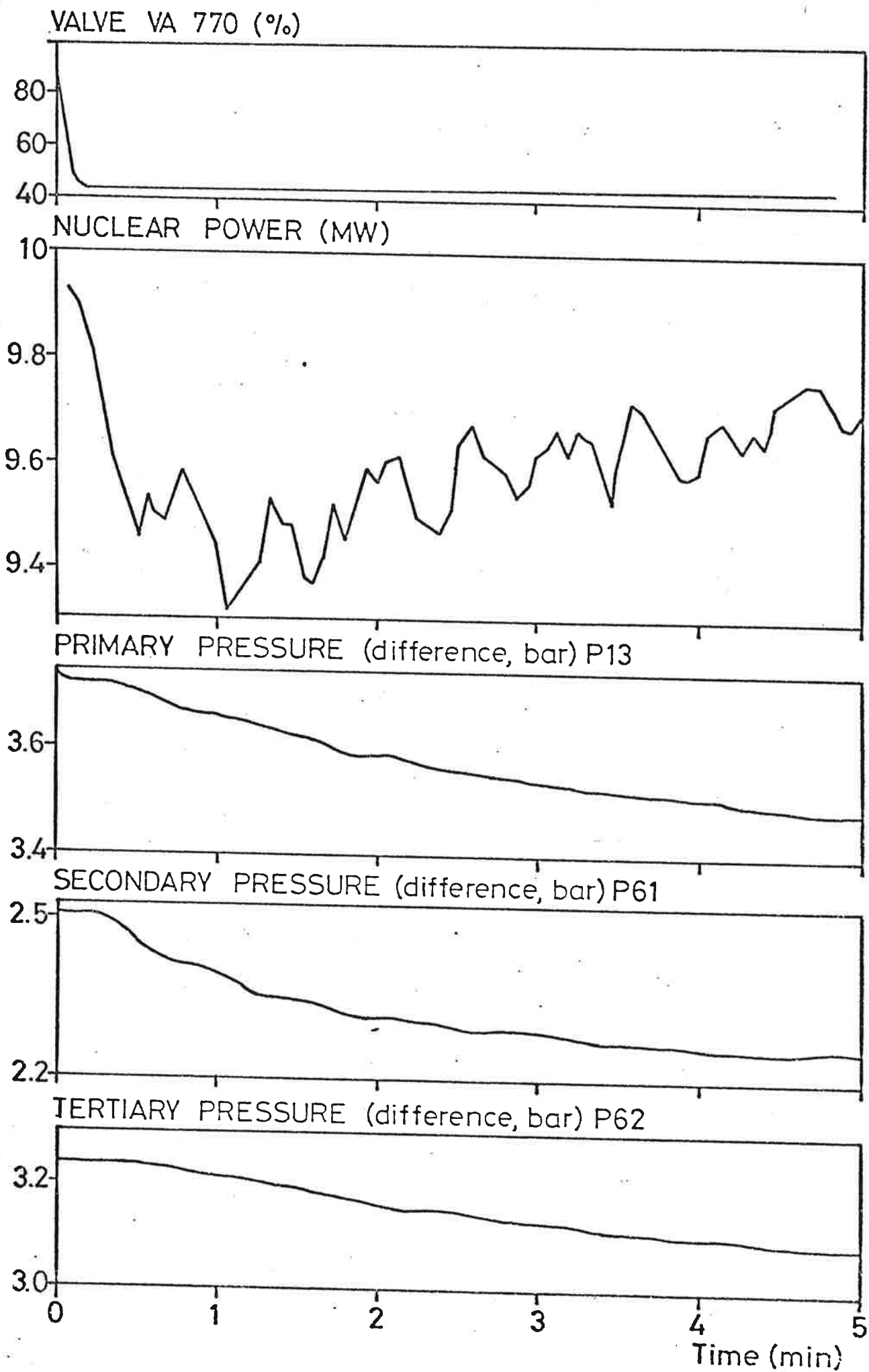


Fig. 5. Typical responses to a step change in  $u_1$ .

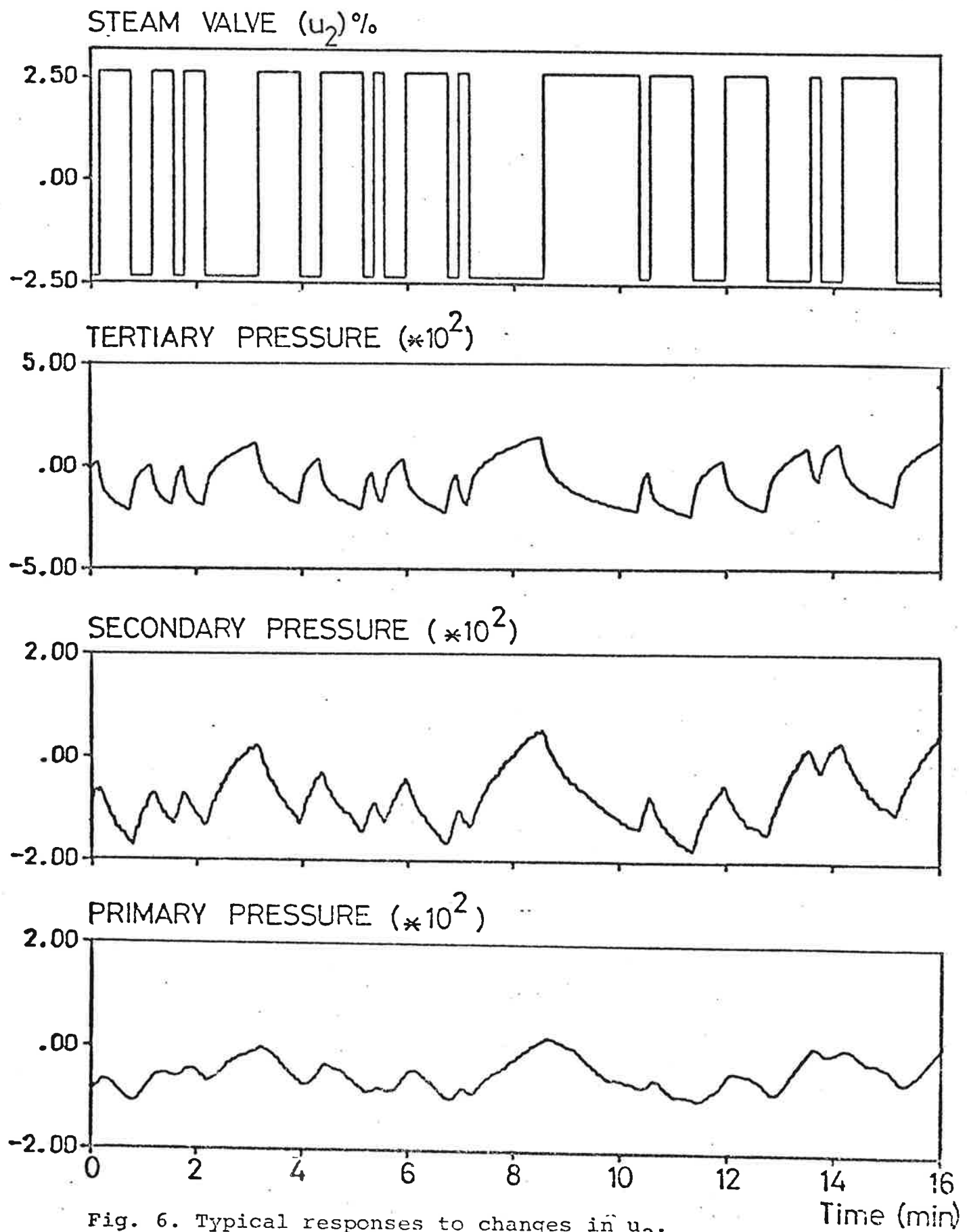


Fig. 6. Typical responses to changes in  $u_2$ .

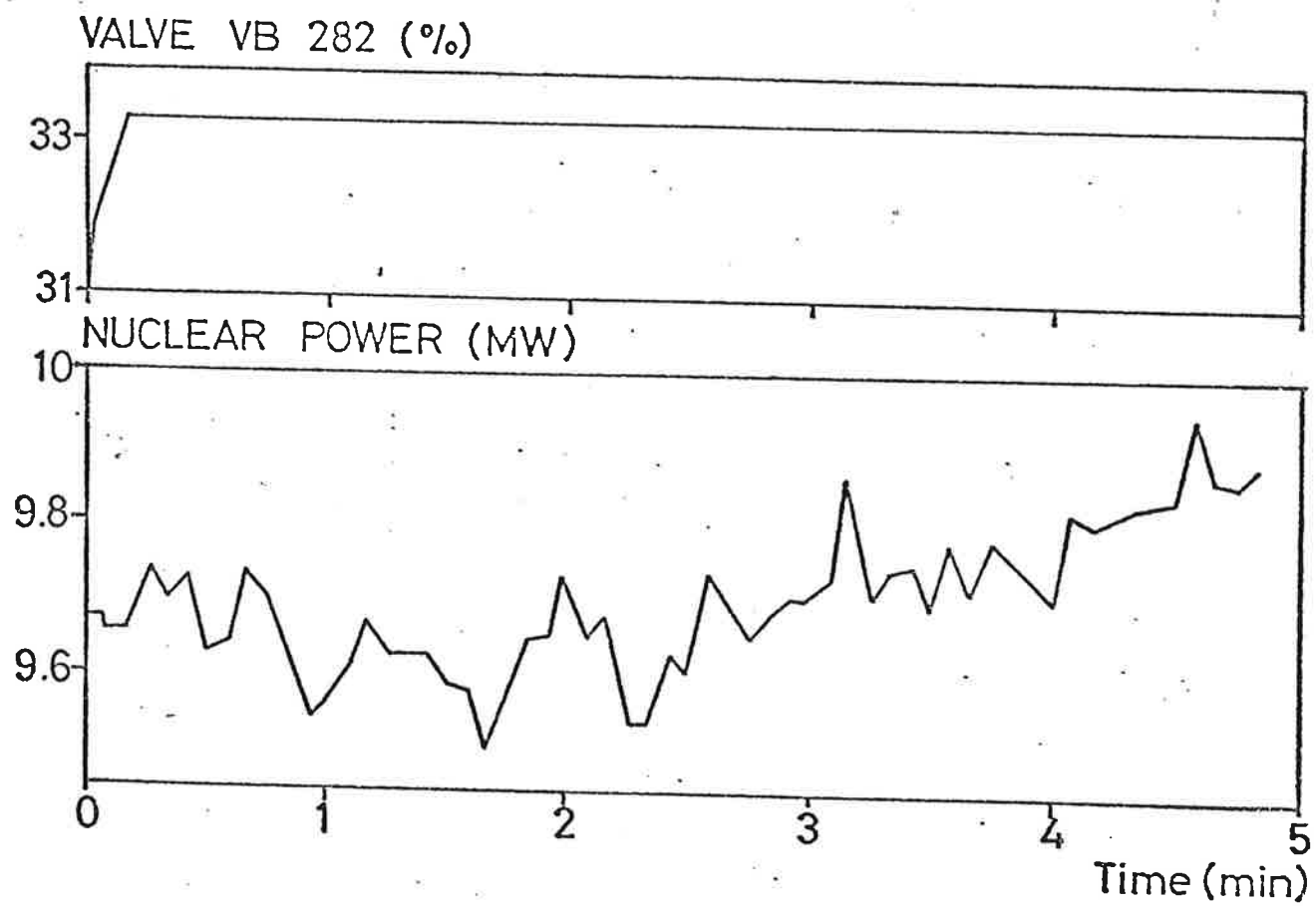


Fig. 7. Nuclear power response to step change in  $u_2$ .



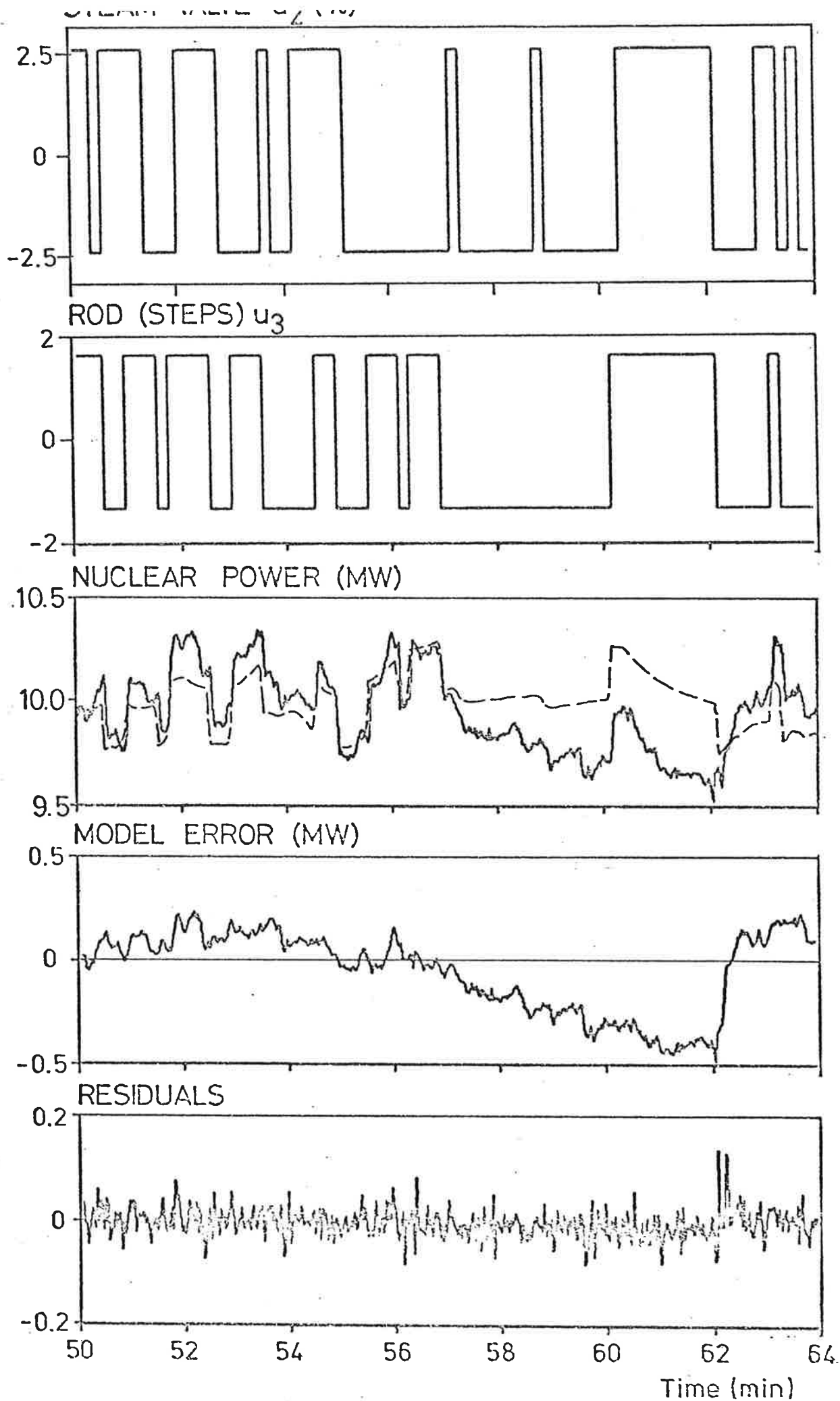


Fig. 8. Model of the nuclear power (broken line) related to  $u_2$  and  $u_3$ . The observed values are from a part of expt 3.

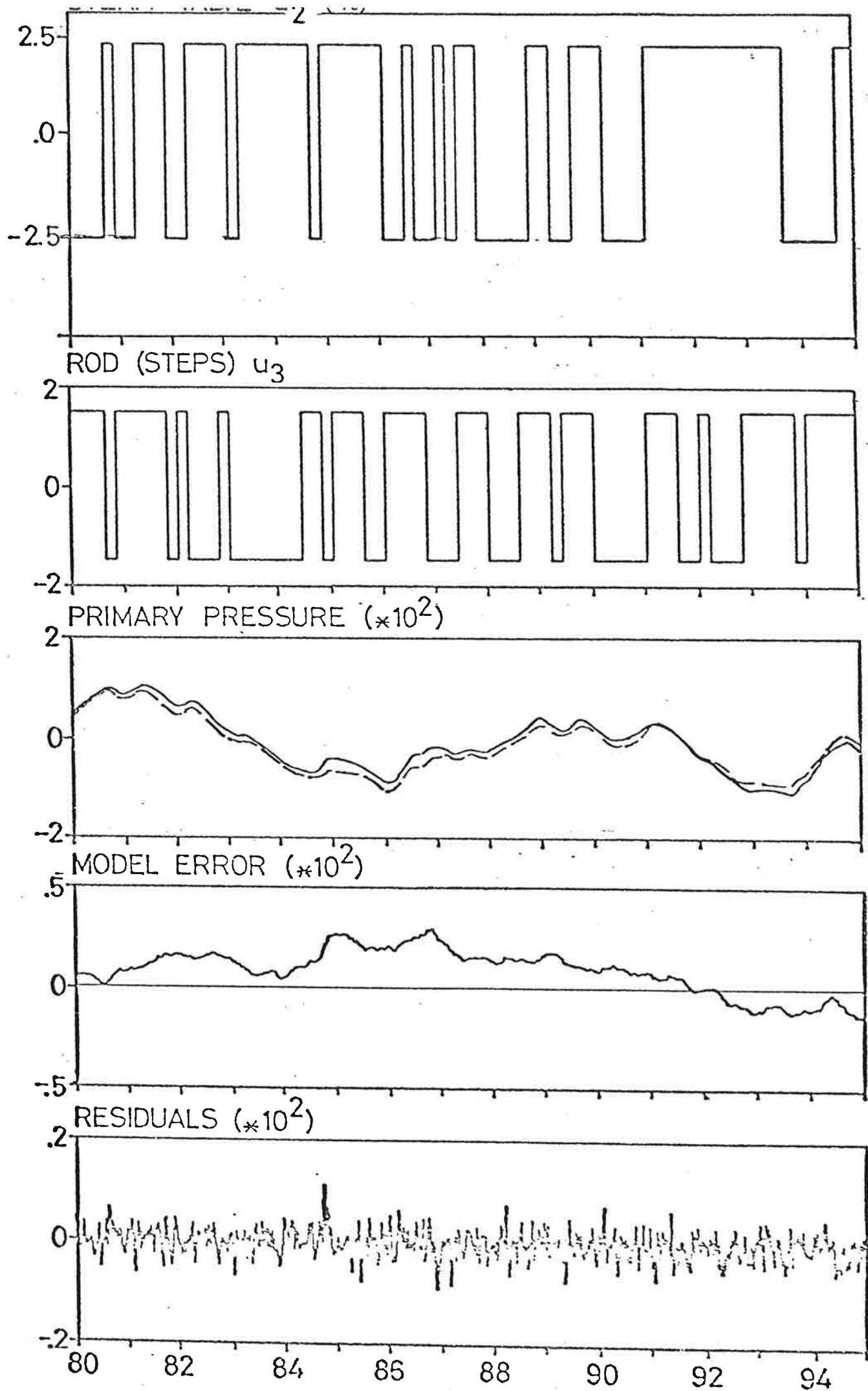


Fig. 9. Model of the primary pressure (broken line) related to  $u_3$  and  $u_2$ . The observed values are from a part of run 2.

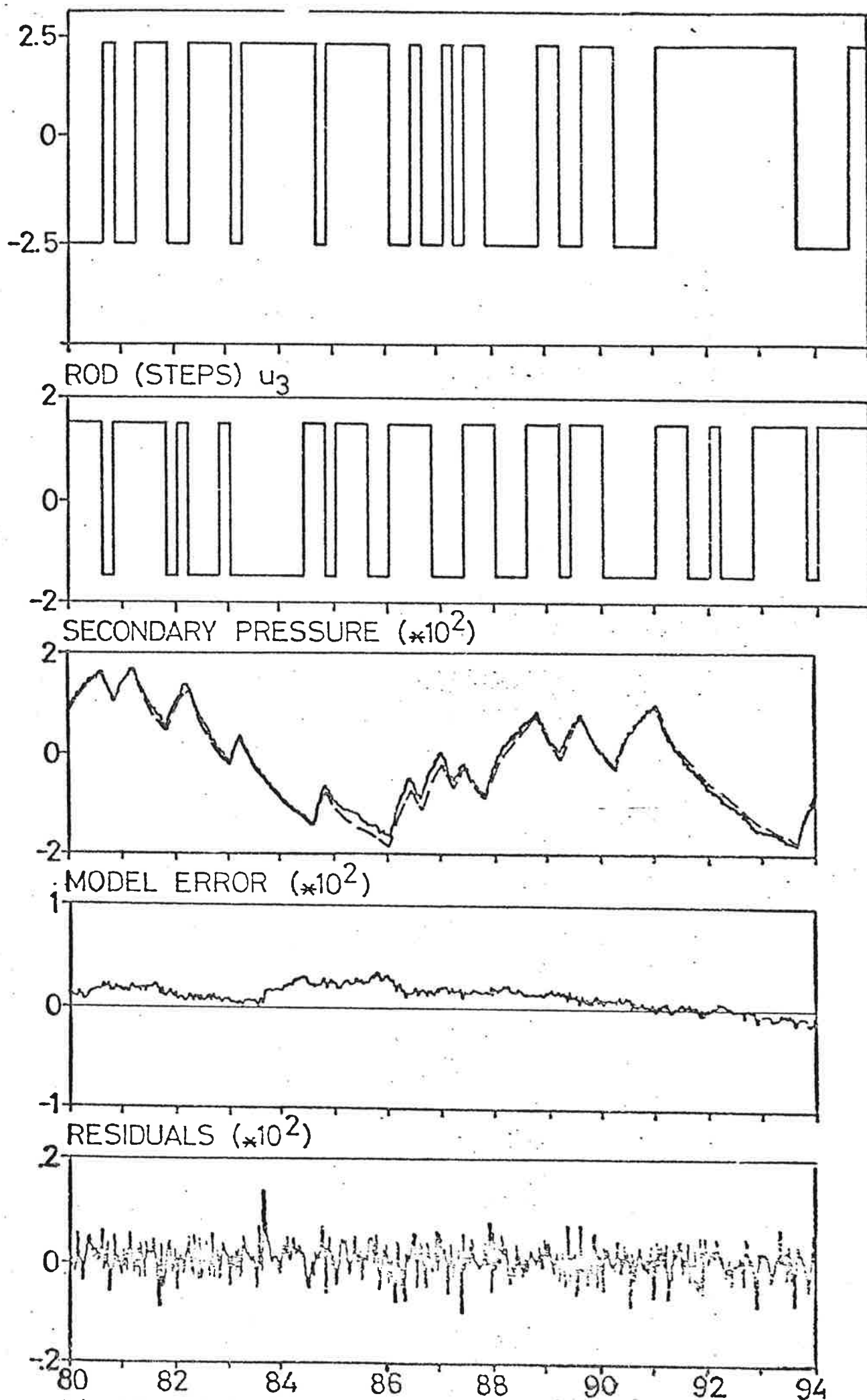


Fig.10. Model of the secondary pressure (broken line) (min) related to  $u_2$  and  $u_3$ . The observed values are from a part of expt. 2

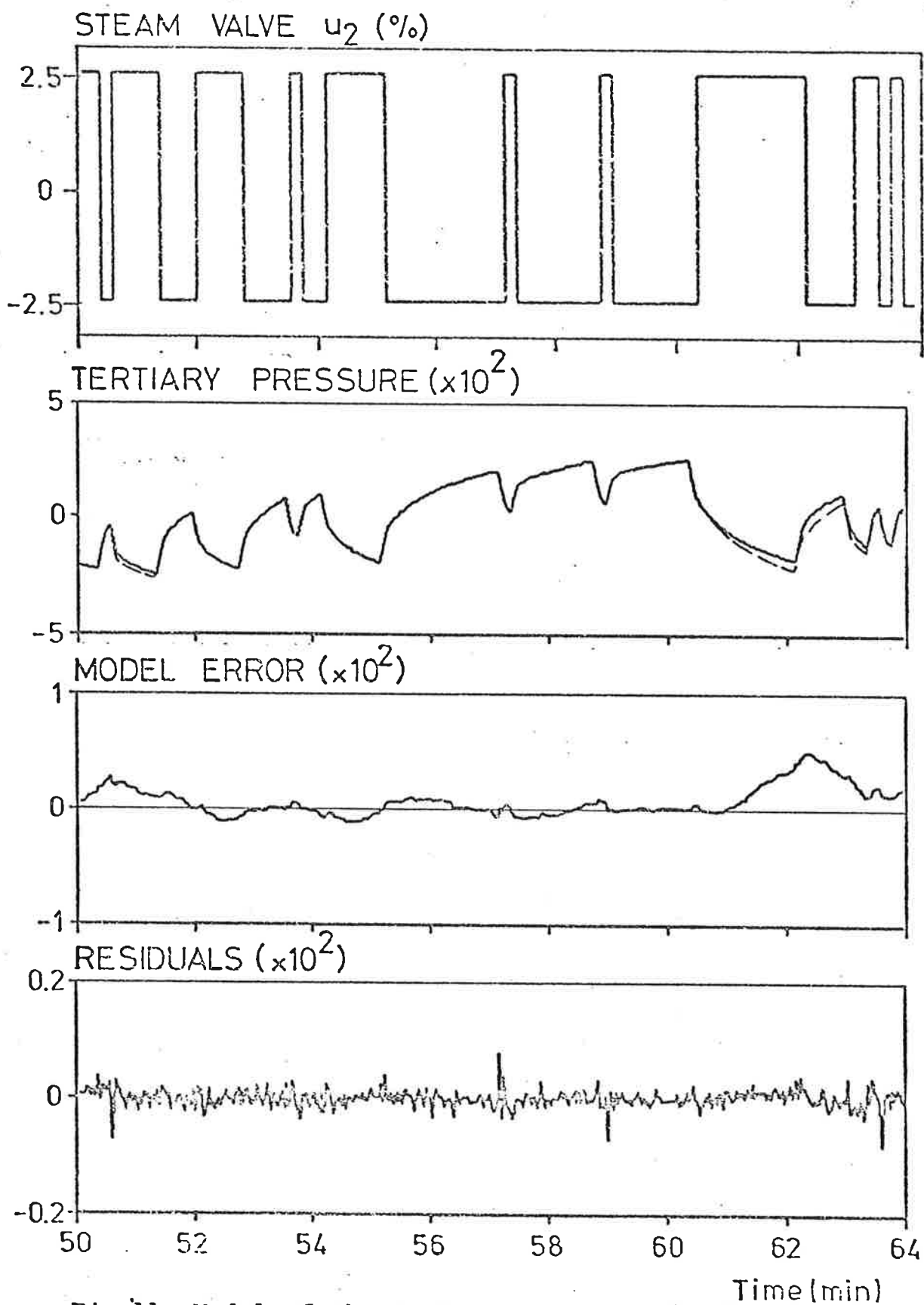


Fig.11. Model of the tertiary pressure (broken line) related to  $u_2$ . The observed values are from a part of expt 3.

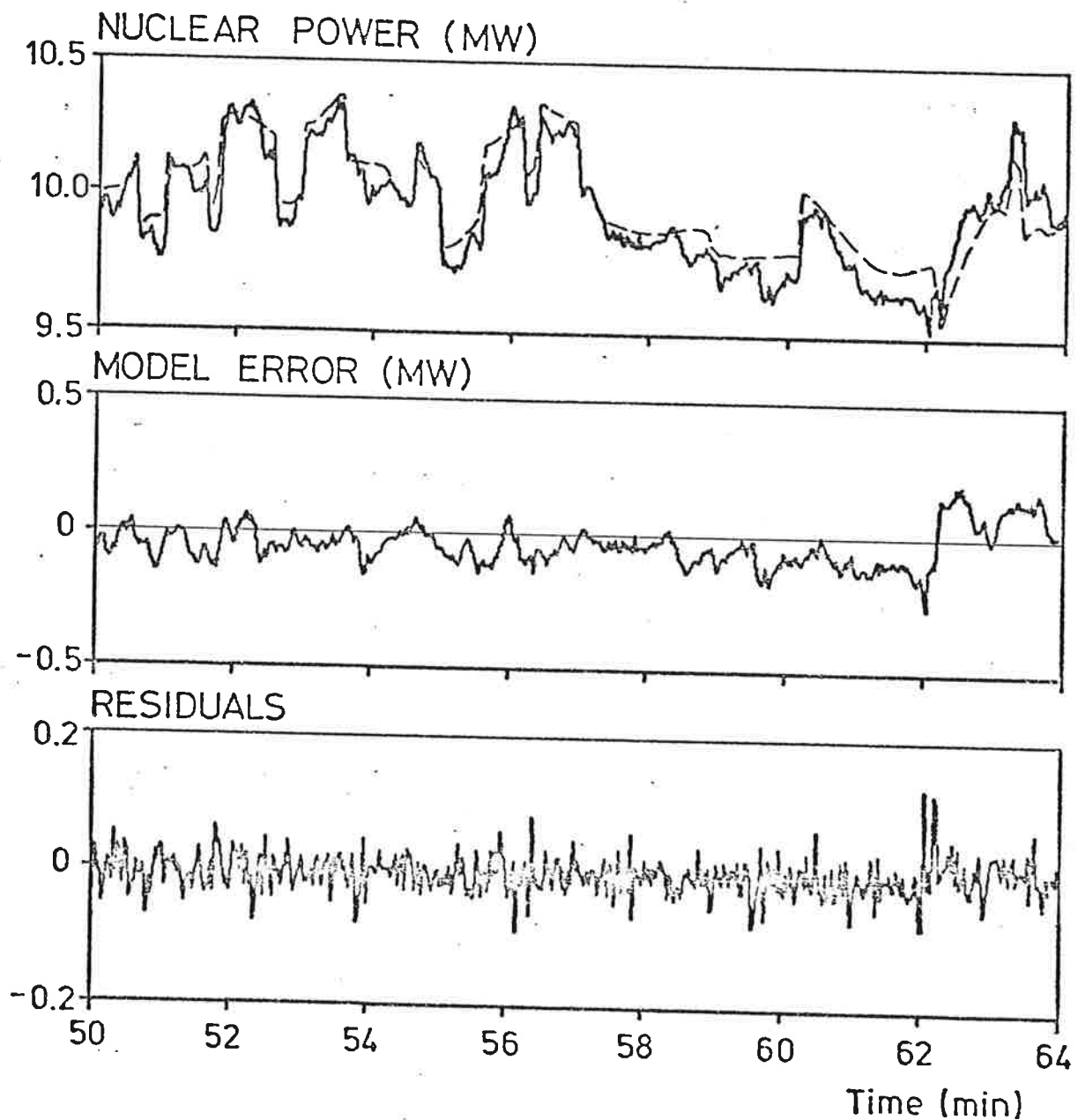


Fig.12. Model of the nuclear power (broken line) related to  $u_2$ ,  $u_3$  and the primary pressure. The observed values are from part of expt 3.

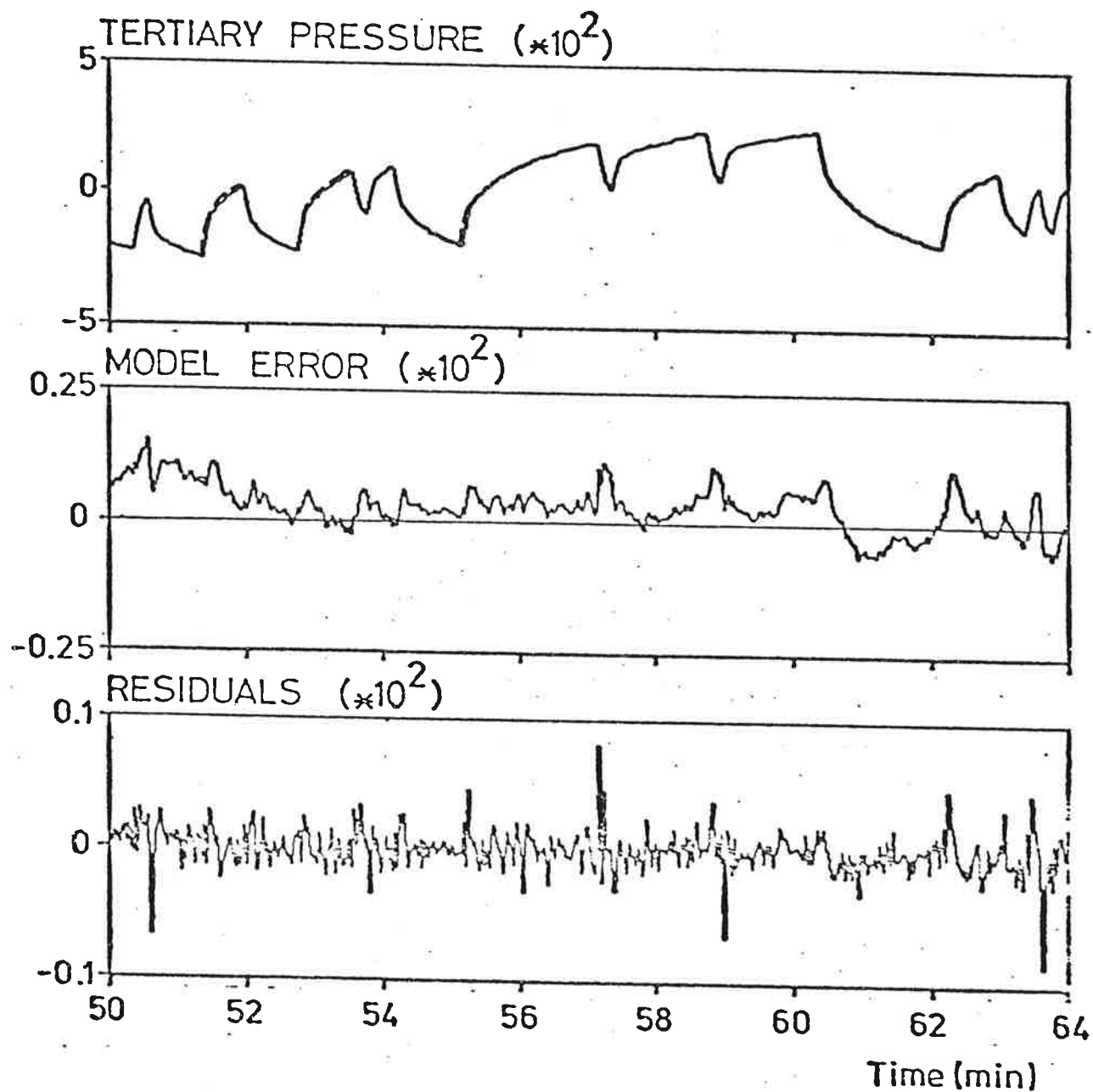
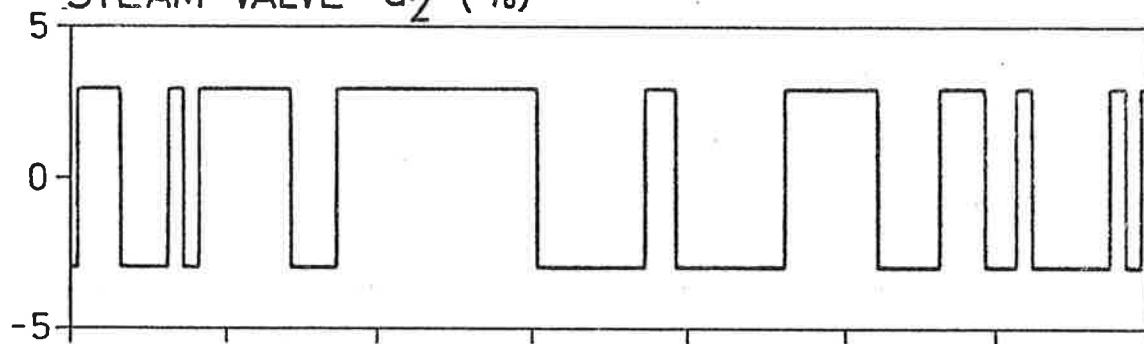
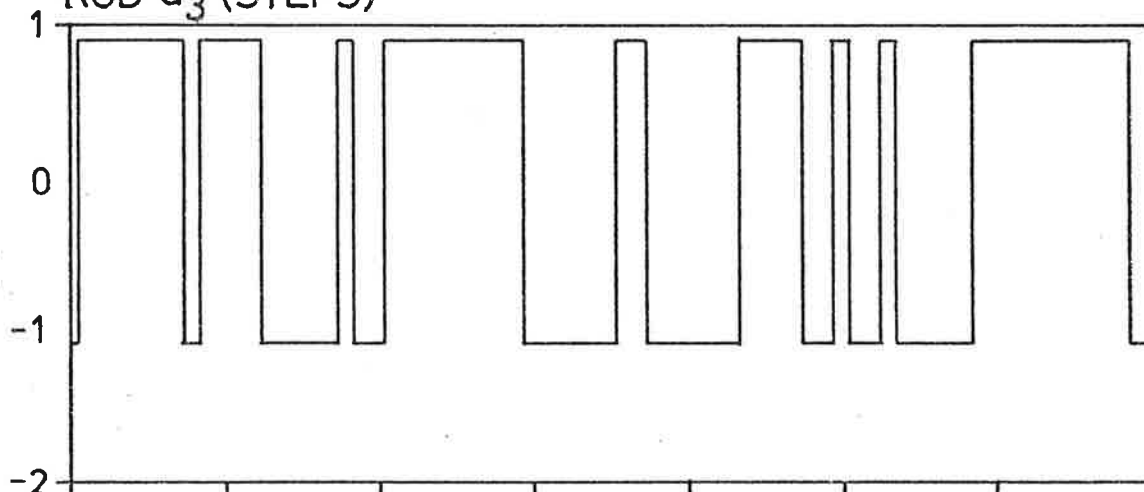
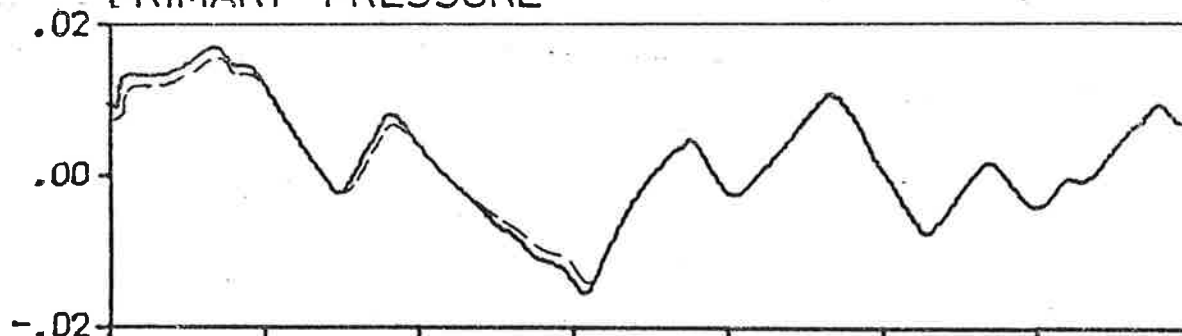


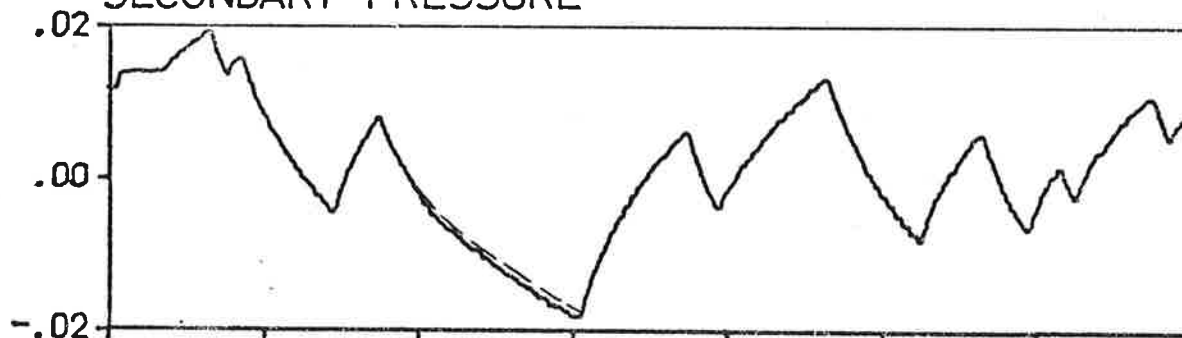
Fig. 13. Model of the tertiary pressure (broken line) related to  $u_2$  and the secondary pressure. The observed values are from a part of expt 3.

STEAM VALVE  $u_2$  (%)ROD  $u_3$  (STEPS)

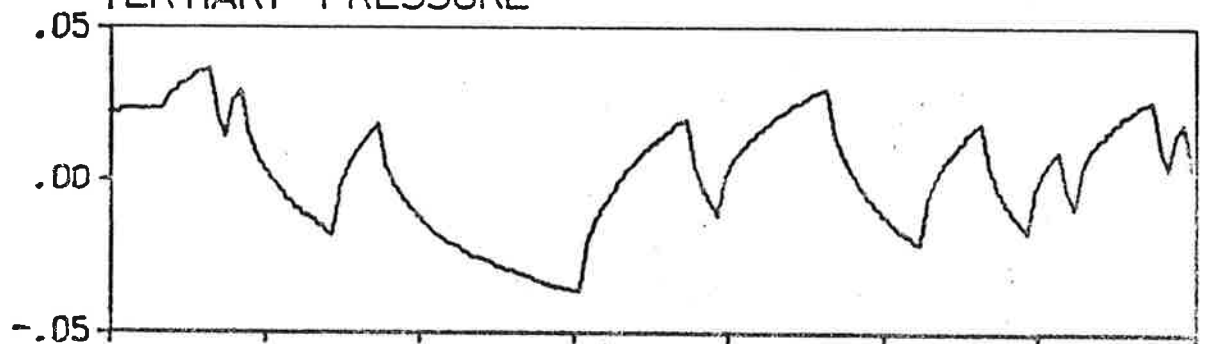
PRIMARY PRESSURE



SECONDARY PRESSURE



TERTIARY PRESSURE



Time (min)

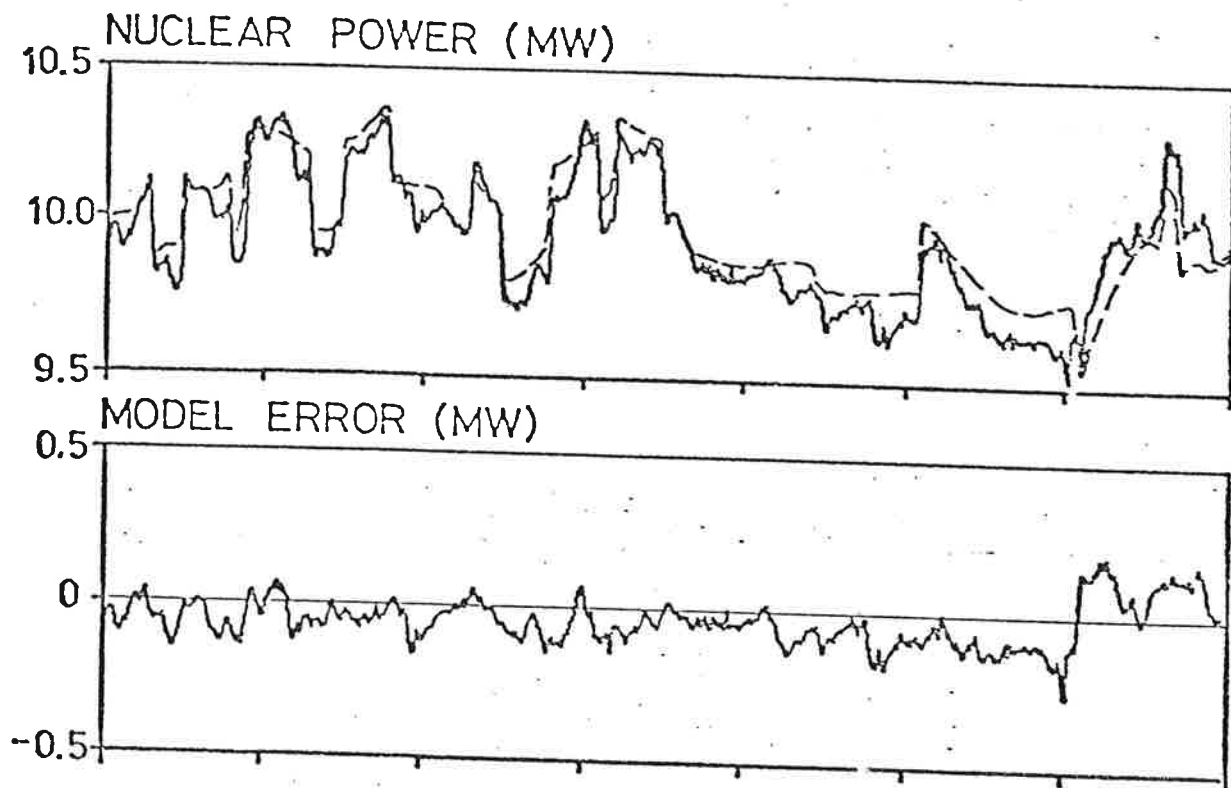


Fig. 14. Nuclear power output from the VDE simulation.  
A part of expt 3 is shown.

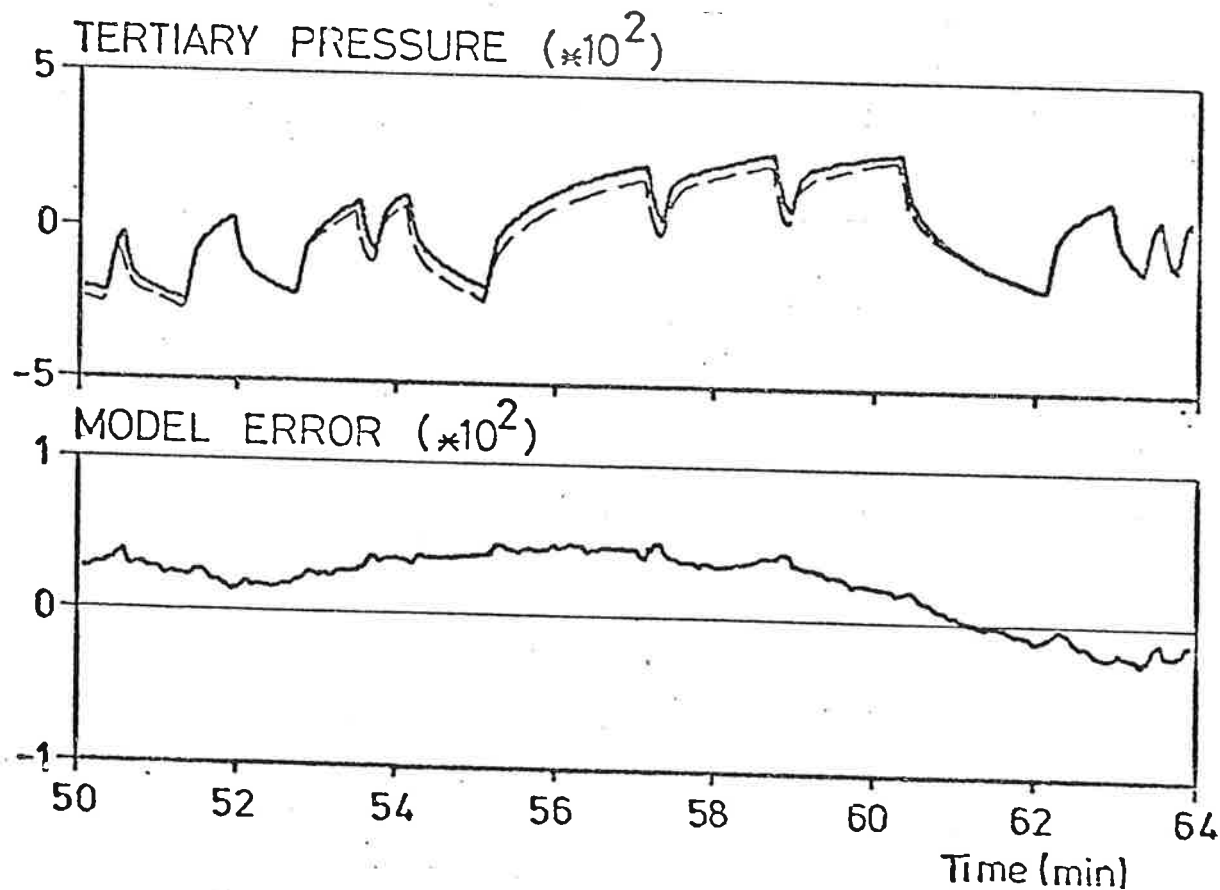


Fig. 15. Tertiary pressure output from the VDE simulation.  
A part of expt 3 is shown.



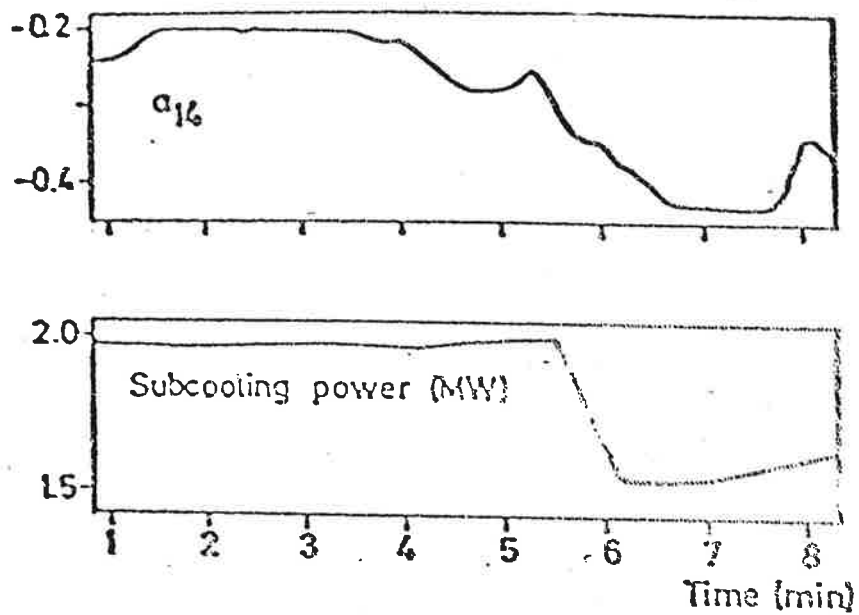


Fig. 17. Estimation of time-varying parameters with the Extended Kalman filter in expt 7. Among the six estimated parameters  $a_{14}$  is shown. The subcooling is changed manually.